ISSN: 1863-5598

ZKZ 64717
04–23

Bodo´s Power Systems®

Electronics in Motion and Conversion

April 2023

PULSED INDUCTANCE MEASUREMENT

POWER CHOKE TESTER DPG10/20 SERIES

Inductance measurement from 0.1 A to 10 kA

KEY FEATURES

Measurement of the

- **Incremental inductance** $L_{inc}(i)$ and $L_{inc}(\int Udt)$
- **Secant inductance** $L_{sec}(i)$ and $L_{sec}(\int Udt)$
- **Flux linkage** $\psi(i)$
- **Magnetic co-energy** $W_{co}(i)$
- **Flux density** $B(i)$
- **DC resistance**

Also suitable for 3-phase inductors

WIDE RANGE OF MODELS

7 models available with maximum test current from 100A to 10000A and maximum pulse energy from 1350J to 15000J

KEY BENEFITS

- Very **easy and fast** measurement
- **Lightweight, small and affordable price-point** despite of the high measuring current up to 10000A
- **High sample rate and very wide pulse width range** => suitable for all core materials

APPLICATIONS

Suitable for all inductive components from **small SMD inductors** to **very large power reactors in the MVA range**

- **Development, research** and **quality inspection**
- **Routine tests** of small batch series and mass production

Technological leader in pulsed inductance measurement for 18 years

www.ed-k.de

Content

Viewpoint 4
Wide Bandgap All the Year!

Events 4

News .... 6 - 14

Product of the Month 16
Monolithic Solution – Power Modules

Blue Product of the Month 18
Field Current Sensor for Electric Vehicle Powertrain Systems

Cover Story .... 20 - 25
Consumer Drives Applications
– Energy Efficiency and Power Density with SiC Power Devices
By Konstantinos Patmanidis, Stefano Ruzza, Claudio Villani, Infineon Technologies

Power Modules .... 26 - 28
Power Modules in Embedded Drives
By Patrick Baginski, Vincotech GmbH, Unterhaching/Germany

Wide Bandgap .... 30 - 32
Easy to Use and Compact: A Family of SiC Power Modules for Automotive Traction Inverters
By Yevgeniy Temko, Philipp Mueller, Anne Bedacht*
**corresponding author, all Robert Bosch GmbH*

Power Conversion .... 34 - 38
How to Optimize Switching Power Supply Layout by Minimizing Hot Loop PCB ESRs and ESLs
By Jingjing Sun, Product Applications Senior Engineer, Ling Jiang, Product Applications Manager, and Henry Zhang, Product Applications Senior Director; Analog Devices

Protection .... 40 - 46
It is Easy to Drive & Protect SiC MOSFET
By Chun Keong Tee, Product Manager of Isolation Products Division, Broadcom Inc.

Thermal Management .... 48 - 51
A Comparative Study of the Thermal Performance of Different Die-Attach Materials Including a Preform-Based Diffusion Solder
By Dmytro Pavlyuchkov & Ralph Mädler, Pfarr Stanztechnik GmbH

Power Quality .... 52 - 55
Power Quality Monitoring Part 1: The Importance of Standards Compliant Power Quality Measurements
By Jose Mendia, Senior Engineer, Product Applications, Analog Devices

New Products .... 56 - 64

Supporters & Friends

A Media
Katzbek 17a
24235 Laboe, Germany
Phone: +49 4343 42 17 90
Fax: +49 4343 42 17 89
info@bodospower.com
www.bodospower.com

Publisher
Bodo Arlt, Dipl.-Ing.
editor@bodospower.com

Editor
Holger Moscheik
Phone + 49 4343 428 5017
holger@bodospower.com

Correspondent Editor Bavaria
Roland R. Ackermann
roland@bodospower.com

Editor China
Min Xu
Phone: +86 156 18860853
xumin@i2imedia.net

US Support
Rusty Dodge
Phone +1 360 920 7825
rusty@eetech.com

Creative Direction & Production
Bianka Gehlert
b.gehlert@t-online.de

Free Subscription to qualified readers
Bodo´s Power Systems is available for the following subscription charges:
Annual charge (12 issues) is
150 € world wide · Single issue is 18 €
subscription@bodospower.com

ASC audit since 09/2006

Printing by:
Westdeutsche Verlags- und Druckerei GmbH; 64546 Mörfelden-Walldorf Germany

Wide Bandgap All the Year!

Regardless of Elon's odd announcement on SiC, we will continue to promote WBG technology because we believe that these materials can and will significantly increase efficiency. That's worth the extra cost to me. I also think that the cost of silicon carbide is not the main reason for Electro Mobility's, let's face it, still stuttering adoption. Or maybe Elon's waiting for some other technology? There's a lot of interesting things about vertical GaN, which is capable of serving the voltage classes of 650 V and above, and thus could become an alternative to SiC. However, it is still wide bandgap, which makes us keep our eyes open for new players in this market.

Staying on topic, we will hold our next WBG Expert Talk at the end of April, followed by one the most important events for power electronics, not just for WBG by the way, PCIM Europe in May. Bodo will once again hold his traditional panel discussion on Wednesday, in the early afternoon. And, you guessed it, there will be two sessions, one on GaN and one on SiC. This year it will be in Hall 7, Booth 480 and Bodo will start with GaN at 1:05 p.m, and the SiC session will start at 2:10 p.m. You won't want to miss this; I can already confirm that we have an excellent speaker list. We could easily have invited double the number of companies to present, but the organizers have put some constraints on us, so I would like to apologize to all of you who will not be able to participate. I sincerely hope that we will still see you in the audience!

But that isn't everything for 2023, there is another highlight in the pipeline: Bodo's annual Wide Bandgap event. After three successful virtual events, it's time to get together in person again. We are currently evaluating the possibilities and are in contact with hotels, caterers, technicians and

so on. Honestly, after the pandemic, it is much harder to get things agreed, but we will do our best to return to what the event stood for, before Covid forced us to go virtual: a gathering of experts in a pleasant environment. Mark your calendars for December 5 and 6, that's the date we're aiming for. Of course, we will keep you informed of any updates here or on our digital channels!

Bodo's magazine is delivered by postal service to all places in the world. It is the only magazine that spreads technical information on power electronics globally. We have EETech as a partner serving our clients in North America. If you speak the language, or just want to have a look, don't miss our Chinese version at bodospowerchina.com. An archive of my magazine with every single issue is available for free at my website bodospower.com.

My Green Power Tip for the Month:
For private households, everybody talks about photovoltaic. But what about wind power? There are initial solutions that are worth considering. At night, the best solar module is useless!

Kindest regards,

Holger Moscheik

Events

PE International 2023
Brussels, Belgium April 18 – 19
www.pe-international.net

FORTRONIC Power 2023
Bologna, Italy April 19 – 20
https://fortronic.it

Battery Tech Expo 2023
Silverstone, UK April 20
www.batterytechexpo.co.uk

Thermal Management Expo 2023
Novi, MI, USA May 1 – 3
www.thermalmanagementexpo.com

PCIM Europe 2023
Nuremberg, Germany May 9 – 11
www.pcim-exhibition.com

Sensor + Test 2023
Nuremberg, Germany May 9 – 11
www.sensor-test.de

SMTconnect 2023
Nuremberg, Germany May 9 – 11
www.smtconnect.com

ICPE 2023 – ECCE Asia
Jeju, Korea May 22 – 25
https://icpe-conf.org

CWIEME Berlin 2023
Berlin, Germany May 23 – 25
https://berlin.cwiemeevents.com

Acquisition of Canadian Gallium Nitride Pioneer

Infineon Technologies and GaN Systems announced that the companies have signed a definitive agreement under which Infineon will acquire GaN Systems for US$830 million.

“GaN technology is paving the way for more energy-efficient and CO 2-saving solutions that support decarbonization. Adoption in applications like mobile charging, data center power supplies, residential solar inverters, and onboard chargers for electric vehicles is at the tipping point, leading to a dynamic market growth,” said Jochen Hanebeck, CEO of Infineon. “The planned acquisition of GaN Systems will significantly accelerate our GaN roadmap, based on unmatched R&D resources, application understanding and customer project pipeline. Following our strategy, the combination will further strengthen Infineon’s leadership in Power Systems through mastery of all relevant power technologies, be it on silicon, silicon carbide or gallium nitride.”

Jim Witham, CEO of GaN Systems, said: “The GaN Systems team is excited about teaming up with Infineon to create highly differentiating customer offerings, based on bringing together complementary strengths. With our joint expertise in providing superior solutions, we will optimally leverage the potential of GaN. Combining GaN Systems’ foundry corridors with Infineon’s in-house manufacturing capacity enables maximum growth capability to serve the accelerating adoption of GaN in a wide range of our target markets. I am very proud of what GaN Systems has accomplished so far and cannot wait to help write the next chapter together with Infineon. As an integrated device manufacturer with a broad technology capability, Infineon enables us to unleash our full potential.”

www.infineon.com

Sales Partnership Expands International Sales Channels

New sales opportunities for Isabellenhütte: Digi-Key Electronics is a global electronic distributor and since October 2022 has offered customers the complete Isabellenhütte range of precision measurement solutions plus precision and power resistors. This collaboration with global reach is between the Isabellenhütte USA subsidiary and Digi-Key Electronics. This distributor offers the entire catalog of standard products from Isabellenhütte, including components for battery management systems, power grids, vehicle electrification, drones and unmanned aircraft, space applications, industrial plants, household appliances and medical equipment. Isabellenhütte’s measurement solutions are in demand wherever there is a need for compliance and precise monitoring of strict power limits in innovative designs.

“Signing a partnership with one of the world’s largest distributors of dispatch-ready electronic components is a huge step forwards for our company”, says Uwe Keller, Managing Director of Isabellenhütte USA. “Our customers will benefit from Digi-Key’s established supply chains. This will allow us to significantly expand our market presence and offer customers greater reliability and improved service.”

The distributor sees Isabellenhütte’s products as an asset in the Digi-Key marketplace. Thanks to extensive experience in metallurgy, Isabellenhütte is able to develop high-quality products with excellent vertical integration, helping customers produce cutting-edge technology.

www.isabellenhuette.de

Silicon Carbide Power Modules Selected for 800V Inverter

British engineering and technology pioneer McLaren Applied has selected STMicroelectronics as a key supplier of silicon carbide (SiC) power modules for its IPG5 800V inverter.

Electric vehicle (EV) powertrain technology increasingly relies on a reliable supply of quality SiC semiconductors such as MOSFETs, especially in 800V architectures. In choosing ST’s SiC, McLaren Applied aims to secure a solid and regular power electronics supply chain for McLaren Applied as it ramps up production and commercialisation of its IPG5 inverter for OEMs and Tier 1 partners.

In the last six months, McLaren Applied has finalised powertrain agreements with American hybrid sports car marque Czinger and in-wheel motor specialists Elaphe for the supply of its IPG5 inverter, with a host of other mid- and high-volume EV models expected to be announced in the near future.

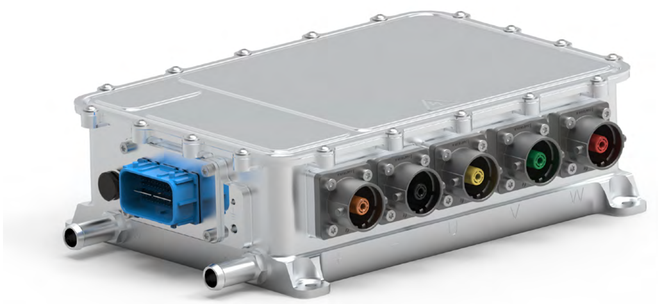

At just 3.79L in size and weighing 5.5kg, IPG5 can extend an EV’s range by over 7%. Derived from decades of innovation in top tier automotive and motorsports applications, McLaren Applied’s IPG5 is highly controllable, offering variable switching frequencies and unparalleled motor response. The variability in switching frequency up to 32kHz enables engineers to use a faster, more efficient, and lightweight drivetrain. McLaren Applied’s IPG5 leverages the ST ACEPACK™ DRIVE power module based on third generation 1200V SiC MOSFET technology.

www.mclarenapplied.com

Test and Measurement Equipment from Oscilloscopes to Bench Power Supplies and Multimeters

RS Group has announced it has significantly expanded the availability of its range of products from Keysight Technologies. Keysight offers a broad range of electronic test and measurement equipment for industrial applications. These include benchtop power measurement and supply, bench multimeters and accessories, oscilloscopes, signal generators and electronic loads, as well as handheld electrical test equipment.

RS has been a long-term distribution partner of Keysight and during the past 18 months, RS has continued to grow its range of Keysight products by more than 600 new products and devices, now available across the EMEA area. RS and Keysight also work closely together across several areas of customer engagement including direct client contact and marketing communications programmes.

A key product offering is Keysight's 'Smart Bench Essentials', which is a package of benchtop test equipment that includes a digital multimeter, power supply, function generator and oscilloscope, plus application software that quickly enables engineers to connect in unprecedented ways. Another key product is the InfiniiVision range of oscilloscopes that deliver leading-edge performance to enable the capture of rare anomalies and glitches with industry-leading waveform update rates or quickly isolate signal events using the range's Zone Touch triggering capability.

www.rs-online.com

Building HQ and GaN-on-SiC Epiwafer Production Facility

SweGaN is to build a headquarters including a high-capacity semiconductor production facility in Linköping. The facility will be built at the Innovative Materials Arena (IMA), a cluster for innovative materials located in Linköping in Östergötland – a region renowned for its progressive materials industries.

Completion of the project is planned for the end of second-quarter 2023 with deployment of the company's manufacturing processes to produce GaN-on-SiC engineered epiwafers in high volume to achieve economies of scale. The facility has been designed to accommodate production capacity up to 40,000 100mm/150mm epiwafers per year.

This significant scaling initiative is backed by a Series A financing round announced in September 2022, and is closely aligned with the accelerated global demands for GaN-on-SiC epiwafers used in 5G base-stations, defense radars, low-orbit satellite communications, and power switches for electric vehicles (EVs). "A new order is being established for semiconductor supply chains, and we are striving to be a go-to strategic partner for our customers in this new era," says CEO Jr-Tai Chen. "Harnessing the challenges and opportunities associated with the new era of semiconductor manufacturing, SweGaN's vision has become clearer than ever – to build a sustainable, smart and green manufacturing for the materials that can enhance connectivity, security, and mobility of the future."

www.swegan.se

Wafer Plant to Boost SiC Power Semiconductor Business

Mitsubishi Electric Corporation announced that it will double a previously announced its investment plan to approximately 260 billion yen in the five-year period to March 2026 mainly for constructing a new wafer plant to increase production of silicon carbide (SiC) power semiconductors. Under the plan, Mitsubishi Electric expects to respond to rapidly increasing demand for SiC power semiconductors for electric vehicles as well as expanding markets for new applications that require, for example, low energy loss, high temperature operation or high-speed switching. The plan will also enable Mitsubishi Electric to contribute to the global green-transformation trend toward energy conservation and decarbonization.

A major portion of the increased investment, approximately 100 billion yen, will be used to construct a new 8-inch SiC wafer plant and enhance related production facilities. The new factory, which will incorporate an owned facility in the Shisui area of Kumamoto Prefecture, will produce large-diameter 8-inch SiC wafers, introduce a clean room featuring state-of-the-art energy efficiency and high-level automated production efficiency. In addition, the company will enhance its production facilities for 6-inch SiC wafers to meet growing demand in this sector as well.

In addition, Mitsubishi Electric will newly invest approximately 10 billion yen in a new factory that will consolidate existing operations, currently dispersed throughout the Fukuoka area, for the assembly and inspection of power semiconductors. The integration of design, development and production technology verification

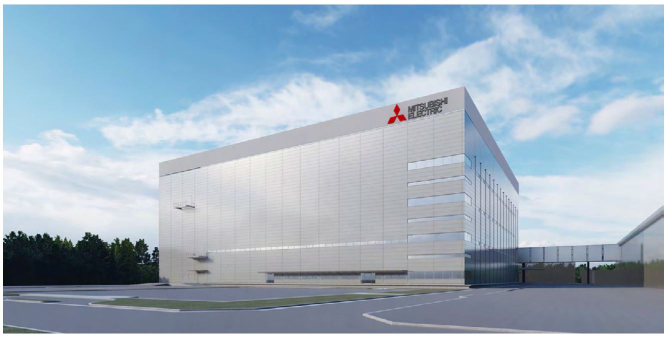

will greatly enhance the company's development capabilities and facilitate timely mass production in response to market demand. The remaining 20 billion yen, all new investment, will be targeted at equipment enhancements, environmental arrangements and related operations.

Over the years, while having led the SiC power module market in fields such as home appliances, industrial equipment and railcars, including the world's first SiC power modules for air conditioners and high-speed trains, Mitsubishi Electric has accumulated extensive expertise in high-performance, high-reliability technologies for screening and many other facets of the SiC power semiconductor production.

www.mitsubishielectric.com


HITACHI
Inspire the Next
Go green+
Get more from your machine
High Voltage IGBT, Hybrid & SiC MOS
High density • Low loss • High cycling
Efficient • Effective • Enabled
pdd@hitachi-eu.com
+44 1628 585151
pdd.heu.eu

300mm Smart Power Fab in Dresden

Infineon Technologies AG is starting construction of its plant for analog/mixed-signal technologies and power semiconductors. After extensive analysis, the Infineon Management Board and supervisory bodies gave the green light for the Dresden site. The German Federal Ministry for Economic Affairs and Climate Action (BMWK) has approved an early project launch, meaning that construction can already begin before completion of the inspection of legal subsidy aspects by the European Commission. Subject to the European Commission's state aid decision and the national grant procedure, the project is to be funded in accordance with the objectives of the European Chips Act. Infineon is seeking public funding of around one billion euros. The company plans to invest a total of approximately five billion euros in the plant, which is set to begin production in 2026. This constitutes the largest single investment in the company's history.

"We're picking up the pace by expanding our production capacities in order to leverage the growth opportunities which the megatrends decarbonization and digitalization are offering us," says Infineon CEO Jochen Hanebeck. "We see structurally growing demand for semiconductors, for example for use in renewable energies, data centers and electro-mobility. By building the 300mm Smart Power Fab in Dresden we are establishing the prerequisites necessary to successfully meet the rising demand for semiconductor solutions."

The plant will be closely linked with the Infineon Villach site as "One Virtual Fab". This manufacturing complex for power electronics based on highly efficient 300-millimeter technology will increase efficiency levels and give Infineon additional flexibility in order to supply its customers faster.

www.infineon.com

Pierre-Francois Allaire Appointed Executive General Manager

Jean Bélanger, CEO and CTO, and Lise Laforce, Executive Vice President of OPAL-RT TECHNOLOGIES, are pleased to announce Pierre-François Allaire as the newly appointed Executive General Manager, effective March 15, 2023. As EGM, Pierre-François will lead all departments and take ownership of daily operations at the company. Jean Bélanger will continue as President and CTO to ensure technology remains the backbone of OPAL-RT's global strategy. Pierre-Francois holds a bachelor's degree in electrical engineering and an MBA. He has more than 19 years of experience within OPAL-RT, including 18 years leading sales and marketing, operations, and support. His 360° vision and in-depth understanding of the business, OPAL-RT's products, and the market have enabled him to play a decisive role in the company's growth and performance, both locally and internationally.

"I have been working at OPAL-RT for the past 20 years and I fell in love with HIL simulation right from the get-go. Today, at 43 years old, I've taken a moment to appreciate what an honor it's been to work and learn at OPAL-RT and make it my home and my family" said Pierre-François Allaire, Sales and Marketing Vice President of OPAL-RT TECHNOLOGIES. "What Jean Bélanger and Lise Laforce have built is truly incredible and I am proud to be part of a company that stimulates innovation and promotes Quebec engineering worldwide. I will bring all my energy to this new position and am fully committed to carrying out OPAL-RT's mission and vision."

www.opal-rt.com

Building Next Wafer Fab in Lehi, Utha

Texas Instruments announced plans to build its next 300-millimeter semiconductor wafer fabrication plant (or fab) in Lehi, Utah. The fab will be located next to the company's existing 300-mm semiconductor wafer fab in Lehi, LFAB. Once completed, TI's two Lehi fabs will operate as a single fab. "This new fab is part of our long-term, 300-mm manufacturing roadmap to build the capacity our customers will need for decades to come," said Haviv Ilan, TI executive vice president and chief operating officer, and incoming president and chief executive officer. "Our decision to build a second fab in Lehi underscores our commitment to Utah and is a testament to the talented team there who will lay the groundwork for another important chapter in TI's future. With the anticipated growth of semiconductors in electronics, particularly in industrial and automotive, and the passage of the CHIPS and Science Act, there is no better time to further invest in our internal manufacturing capacity."

The landmark $11 billion investment marks the largest economic investment in Utah history. The Lehi expansion will create approximately 800 additional TI jobs as well as thousands of indirect jobs. TI looks forward to strengthening its partnership with the Alpine School District and will invest $9 million to improve student opportunities and outcomes.

www.ti.com

Small-IPM Series – 2nd Generation

Ideal for Air Conditioners, Inverters and Servo Systems

MAIN FEATURES

- Reduction of losses and improvement of energy efficiency by utilizing 7th generation IGBT technology
- Built-in gate driver IC for optimum switching conditions
- Expansion of permissible operating area by improving the accuracy of overcurrent and overheating protection functions
- Utilizes an ultra-small DIP package with high heat dissipation aluminium insulating substrate

An IPM is a module which include three-phase inverter bridge circuit, control circuit and protection circuits.

Comparison with previous generation

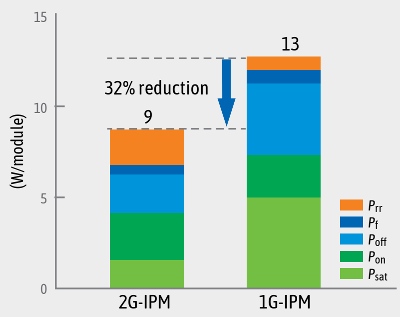

$I_{O\,(RMS)} = 3$ A, $V_{DC} = 325$ V, $f_O = 60$ Hz, $f_c = 5$ kHz,
$\lambda = 1.0$, 3 ph-mod, $T_c = 100$ °C

Estimated loss of a 10 hp PAC at intermediate load
650V / 50 A rating

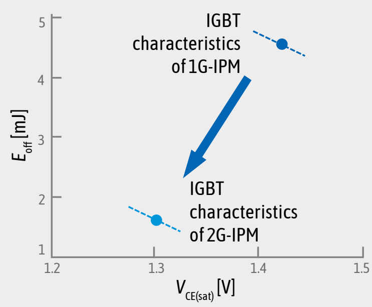

$V_{CE(sat)}$ — E_{off} trade-off

www.fujielectric-europe.com
www.americas.fujielectric.com/semiconductors

Fuji Electric
Innovating Energy Technology

Virtual Fab Underpins Strategies to Reduce the Carbon Footprint

imec presents a quantitative assessment of the environmental impact of patterning in advanced IC manufacturing. A virtual fab has been developed in the imec.netzero modeling platform. The resulting analysis enables imec and its partners to assess current manufacturing choices, identify areas of focus, and project the future. In imec's physical fab, environmentally friendly process solutions are explored for the high impact areas, which include the reduction of fluorinated etch gases, maximizing EUV scanner throughput, and reducing hydrogen and water consumption.

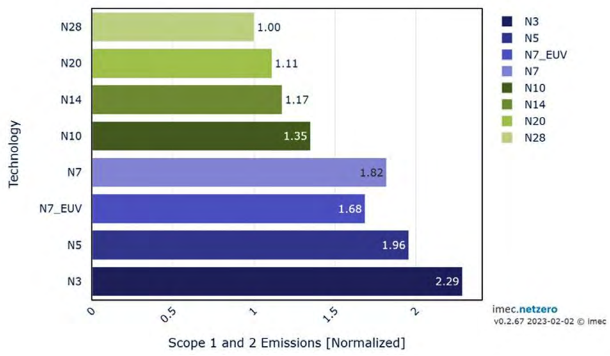

CO2 emissions associated with IC manufacturing are expected to quadruple in the next decade, due to both the increasing complexity of advanced technologies and the projected growth of the total volume of wafers produced. To counter this scenario, leading semiconductor players have committed to becoming carbon neutral or net-zero by 2030-2050. In that context, imec launched its Sustainable Semiconductor Technologies and System (SSTS) program, gathering the supply chain to jointly target net-zero emissions for chip manufacturing. One of the goals of SSTS is to offer the industry a unique bottom-up approach that provides actionable data with a high granularity enabling impact assessment during process and flow development.

www.imec-int.com

800V Electric Vehicles Charge into the Mainstream using SiC Power Electronics

The demand for electric vehicle (EV) power electronics will increase dramatically in the next ten years, primarily driven by rapid growth in the BEV car market, where IDTechEx predicts a 15% CAGR globally over the next decade. Currently, the weighted-average battery capacity of BEV cars is increasing in all regions, piling pressure on battery supply chains, and creating uncertainty. The result is that drive cycle efficiency must come to the forefront of powertrain design, meaning the time has come for high voltage wide bandgap (WBG) power electronics. The IDTechEx report "Power Electronics for Electric Vehicles 2023-2033" provides a deep-dive into EV power electronics with technology insights into the evolving semiconductor and package materials, including Si, SiC and GaN semiconductors, die-attach materials, wire bonding, thermal management, and more. IDTechEx presents granular forecasts detailing unit sales, GW and US$ demand for inverters, onboard chargers (OBC) and DC-DC converters segmented by voltage (600V, 1200V) and semiconductor type (Si, SiC, GaN). While Si IGBTs have dominated the

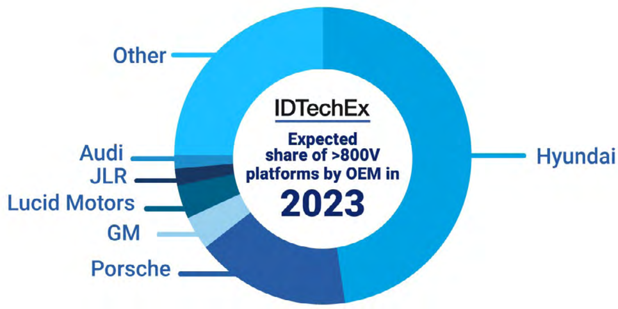

medium-to-high power device range for 20 years, including in EV power electronics, they are giving way to a new generation of WBG materials: SiC and GaN. This will fundamentally impact the design of new power devices, including the package materials, as high voltage and high power-density modules operating at higher temperatures becomes the trend.

www.idtechex.com

Strengthening Sustainable Battery Industry 'Made in Germany'

Setting a sustainable course for the future of the German battery industry: The Customcells company is investing tens of millions in the expansion of its Itzehoe site in Schleswig-Holstein, Germany. The production team on site will be tripled. With more research and innovation as well as joint process development, the specialists for application-specific premium battery cells are boosting Germany's path to becoming an international market leader for green high-performance technology,enabling the mobility revolution thanks to holistic electrification on the road, on water and in the air.

"With the expansion in Itzehoe and the investments we are making here, we are also making a commitment: We believe in Germany as a location for a successful battery industry. We are literally energizing 'Made in Germany' – sustainable, innovative, high-performance, high-tech," Dr. Dirk Abendroth, CEO of the Customcells Group, said while laying the groundwork for the company's expansion at its site in Itzehoe. The experts for premium battery cells are investing tens of millions for the buildings on site alone. During this time, the total number of employees will double.

INVESTING IN LOCATION: CUSTOMCELLS STRENGTHENS SUSTAINABLE BATTERY INDUSTRY 'MADE IN GERMANY'

German and European politicians have recently expressed concerns that the US government's Inflation Reduction Act (IRA) could have consequences for the development of the battery industry in Germany.

www.customcells.org

Expanding Silicon Carbide and Silicon Capacity in Colorado

Microchip Technology announces plans to invest $880M to expand its silicon carbide (SiC) and silicon (Si) production capacity at its Colorado Springs, Colo. manufacturing facility over the next several years. One significant phase of the expansion is to develop and upgrade its 50-acre, 580,000-square-foot Colorado Springs campus for increased SiC manufacturing for use in automotive/E-Mobility, grid infrastructure, green energy, and aerospace and defense applications. The Colorado Springs campus currently employs more than 850 people and produces products from 6-inch wafers. The manufacturing technology that Microchip is installing will run on 8-inch wafers, which will significantly increase the number of chips produced at this location. The additional 400 jobs anticipated at the facility will range from production specialists to technical roles in equipment procurement and management, process control and test engineering.

"With over two-decades of investment in silicon carbide, Microchip's portfolio is designed to provide our customers with innovative power solutions," said Rich Simoncic, senior vice president of Microchip's Analog businesses. "This campus is an integral part of producing our SiC technology to assure our customers with supply certainty as they transition to SiC solutions."

www.microchip.com

Global Distribution Agreement Announced

Vicor announced its distribution agreement with Avnet, which expands access to Vicor's power modules through Avnet's design and supply chain, enabling global customers to achieve innovation with higher system performance and greater scalability.

"This is a great opportunity for Vicor to partner with a global leader aligned with Vicor's target markets," said David Krakauer, VP Industrial Business Unit and Corporate Marketing. "Working with Avnet will better position Vicor to bring our highly differentiated modular power solutions to customers who wish to unleash the power of their own innovations."

"In today's markets, businesses need to innovate to stay ahead of the competition," said Peggy Carrieres, Global Vice President Supplier Development for Avnet. "This agreement comes at a time when many of our customers are looking for opportunities to separate themselves from the pack. They are struggling to fit more power in increasingly smaller spaces, and they are searching for power-dense and highly efficient solutions. Vicor power modules will deliver a quality solution for our customers."

The global franchise agreement is effective immediately. Customers in the EMEA region (Europe, Middle East & Africa) will have access to the Vicor product portfolio via Avnet's European business unit, Avnet Abacus, an interconnect, passive, electro-mechanical and power distributors.

www.vicorpower.com

eBook Explores the Future in Automotive Design

Mouser Electronics announces an eBook in collaboration with Qorvo, highlighting the technology innovations reshaping automotive design. In The Future of Automotive, subject matter experts from Qorvo and Mouser offer rich, practical analyses of technologies including on-board chargers (OBC) for electric vehicles. The automotive industry is currently experiencing a broad range of technological innovations. As automotive manufacturers invest in electric vehicle design, the way in which we power our vehicles is changing. At the same time, new technologies and components are enabling the design of the connected vehicle. These advanced automobiles contain more safety features than their predecessors, while also supporting a variety of new entertainment and information possibilities for those traveling as passengers. The Future of Automotive, the eBook from Mouser and Qorvo, offers a detailed collection of articles exploring the products and solutions underpinning these innovations. The eBook highlights product information for six specific Qorvo solutions, connecting automotive designers to the components that will enable the next generation of automobile designs.

www.mouser.com

Technical Blog Launched

For tenured engineers, power converter datasheets are easily consumed, and many of the technical concepts are well understood. However, through Traco Power's regular interaction with students, it is clear that not all aspects of how power supplies are specified are fully appreciated and immediately comprehendible. With this in mind, Traco Power is launching a technical blog.

"Over the years, ever more parameters have been added to our datasheets to support the requests of our customers," states Florian Haas, Vice President of Marketing & Digitalization, Traco Power Group. "However, we've seen that these parameters are not always clear for engineering graduates and students. Our new technical blog is aimed at all those who wish to delve deeper into the datasheets and fully understand not only the entries they contain, but also why they are important to their application's design."

Drawing upon the Traco Power engineering team's years of experience and reflecting on the questions regularly posed to its engineers, the blog tackles everything from EMC basics and power converter specifications to application-specific challenges.

"We've gathered so many questions and answers over the years, it simply made sense to release this information so as to expand how we support customers," said Andreas Flühler, Head of Technical Services. "The technical blog enables us to provide engineers and students with answers to their queries more efficiently while also making our expanse of power converter knowledge available to everyone who visits our website."

www.tracopower.com

ECPE Events

ECPE Tutorial: EMC in Power Electronics
Cambridge, United Kingdom
19/04/2023 - 20/04/2023

ECPE Tutorial:
High-Precision Power Electronics
Eindhoven, Netherlands
25/04/2023 - 26/04/2023

Registration PhD students | European PhD School on 22 - 26 May 2023 in Gaeta, Italy
Gaeta, Italy
22/05/2023 - 26/05/2023

ECPE Tutorial:
Packaging in Power Electronics
Munich, Germany
23/05/2023 - 24/05/2023

ECPE Lab Course: EMC Optimised Design (Parasitics in Power Electronics)
Berlin, Germany
22/06/2023 - 23/06/2023

ECPE Tutorial:
Thermal Engineering of Power Electronic Systems Part I:
Thermal Design and Verification
Nuremberg, Germany
11/07/2023 - 12/07/2023

ECPE Tutorial: Thermal Engineering of Power Electronic Systems Part II:
Thermal Management and Reliability
Nuremberg, Germany
25/10/2023 - 26/10/2023

www.ecpe.org

Monolithic Solution – Power Modules

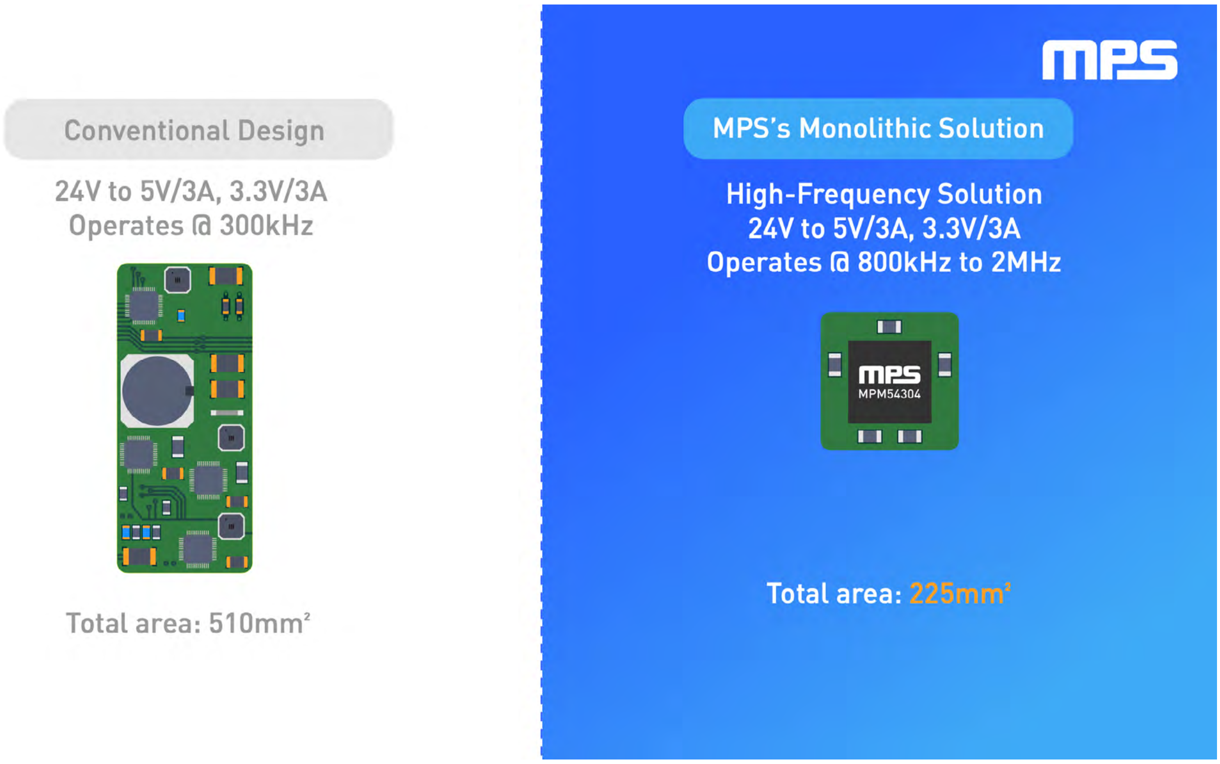

Monolithic Power Systems (MPS) provides a suite of high-performance, all-in-one power modules, which are comprised of controllers, power MOSFETs, and inductors in compact, surface-mount packages. These modules deliver high efficiency, a small form factor, and adjustable performance to accelerate innovation and advance various industries, including industrial, automotive, consumer, and computing.

An example of an MPS power module is the MPM3515, a 1.5A, 36V module, featuring exceptional efficiency and low noise. This module has been designed to operate in harsh environments, making it well-suited for industrial applications that require high efficiency and reliability, such as industrial automation, robotics, and motor control. With unique "silent switcher" technology, the MPM3515 mitigates electromagnetic interference (EMI) concerns. The MPM3515 also operates with a 2.2MHz switching frequency to achieve a fast load transient response, and comes with a full range of protection features, including over-current protection (OCP) and thermal shutdown. With its space-saving QFN-17 (3mmx5mmx1.6mm) package, the MPM3515 eliminates design and manufacturing risks while dramatically improving time-to-market.

With the rise of supercomputing, AI, and 5G networks, the demand for high-current, high-performance power solutions is increasing in various industries. That's why MPS has developed the MPM3695 power module family, a set of high-current modules that are capable of delivering up to 10A to 100A each. For even higher current requirements, these modules allow multi-phase operation with automatic interleaving. Together with their auto-compensation and adaptive multi-phase constant-on-time (MCOT), these advanced features enable ultra-fast transient response, making the MPM3695 family ideal for powering networking systems or devices such as FPGAs and ASIC core power.

Some applications require multiple mid-current rails, which are usually implemented with PMICs, therefore taking up a lot of board space and adding complexity to PCB design, especially in terms of electromagnetic compatibility (EMC). MPS solves this problem thanks to its multiple-output modules, ranging from 2 to 4 regulated outputs. For example, the MPM54304 is a complete power management module that integrates four high-efficiency, step-down DC/DC converters, inductors, and a flexible logic interface. This COT control DC/DC converter provides fast transient response, and its default 1.5MHz switching frequency greatly reduces external capacitor size. This makes the MPM54304 ideal for FPGA power supplies, multi-rail power systems and MCU/DSP power supplies.

For other applications such as optical transceivers, MPS has designed the MPM54313, a triple-output power module that can deliver up to 3A on each rail, making it ideal for meeting QSFP specifications. This module integrates the inductors and output filter components, helping designers easily meet noise immunity and voltage ripple requirements.

MPS modules feature high efficiency, compact dimensions, and adjustable performance, and are available in various power ratings and input/output configurations, making them suitable for a broad range of applications. However, the key advantage about these modules is the design simplicity they provide, allowing a more efficient allocation of design resources, eliminating design risks and significantly cutting time-to-market.

In conclusion, MPS power modules offer several advantages to designers and engineers, including reduced board space, simplified design, improved efficiency, and increased reliability. These modules facilitate high performance and efficiency across a broad range of industrial applications, including industrial automation, robotics, motor control, and power tools.

www.monolithicpower.com

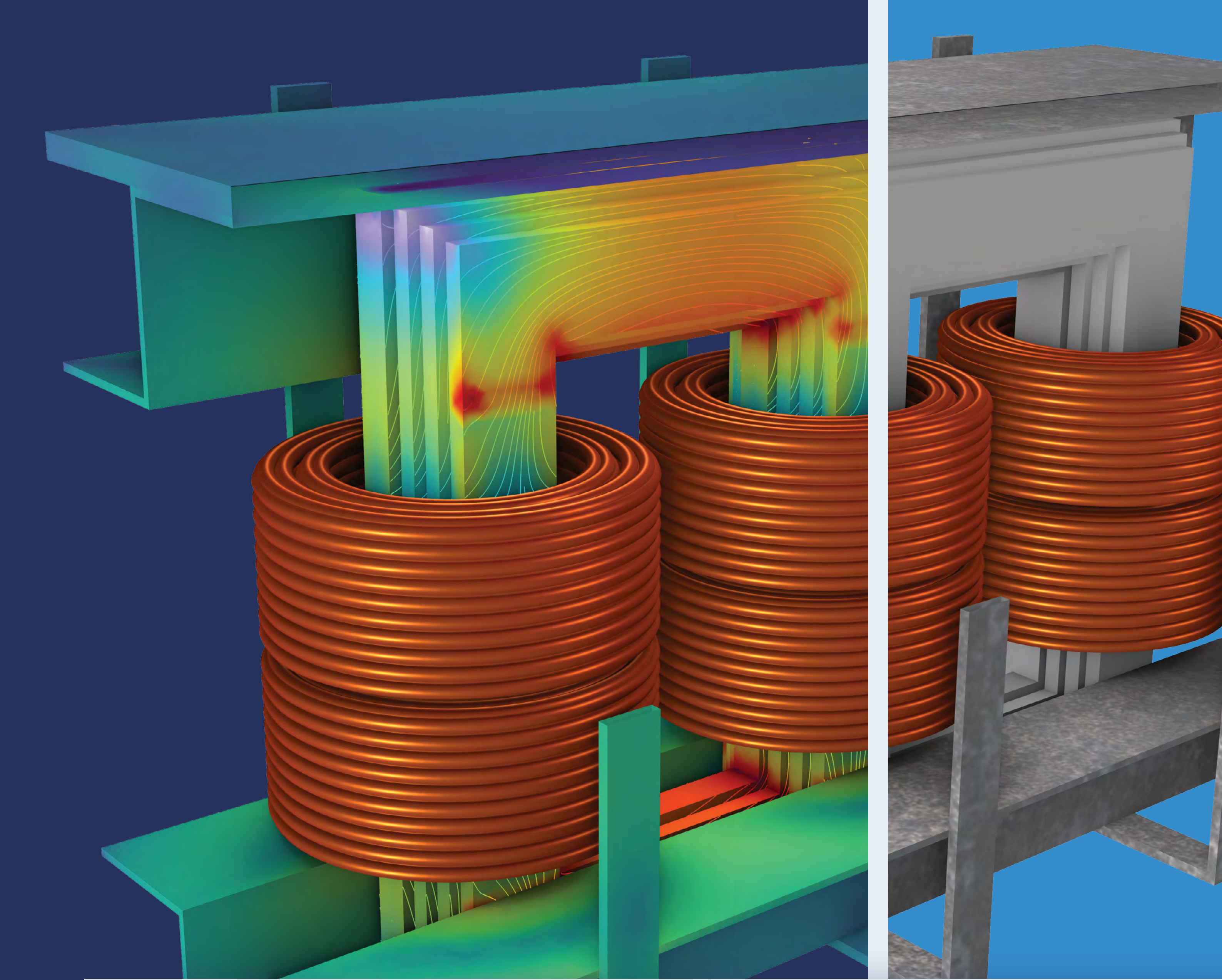

Field Current Sensor for Electric Vehicle Powertrain Systems

Samples are available now to support designers in achieving new safety and efficiency standards

Allegro MicroSystems announces the release of samples for the ACS37601, an ASIL C safety rated, high-precision, field current sensor with for traction and auxiliary inverter systems as well as battery management systems (BMS) in electric vehicles (EVs).

Designers of inverter and battery management systems are challenged to achieve higher safety targets based on new Automotive Safety Integrity Level (ASIL) requirements.

To enable customers to meet these safety requirements, while increasing system efficiency and extending battery life, Allegro has developed the ACS37601 programmable linear Hall-effect current sensor IC with overcurrent, overtemperature, and self-test capabilities. Designed to achieve high accuracy and resolution without compromising bandwidth, the ACS37601 is Allegro's field current sensor for applications requiring measurement capability greater than 200 Amperes.

"Allegro's ACS37601 is enabling us to meet e-mobility functional safety and accuracy requirements in our BMS and EV traction inverter current sensor applications," says Julio Urrea, Vice President of Business Development at Littelfuse, a diversified industrial technology company empowering a sustainable, connected, and safer world in the electronics, transportation, and industrial markets.

To be used along with a C-core, the ACS37601 is the first ASIL C-rated field current sensor that achieves 0.8% sensitivity error and less than 5 mV offset error over the automotive temperature range, and—with 30% less noise than legacy devices—this IC is ideal for battery management applications. The high operating bandwidth from DC to 240 kHz and fast 2 µs response time enable new performance in DC battery charging and high-frequency automotive inverter applications. To support adoption of the most advanced microprocessors without requiring additional components, the ACS37601 works with 5 V or 3.3 V power supplies.

"Littelfuse has a history of excellence as an automotive supplier with a tremendous global footprint. We are excited to work with them to deliver industry-leading magnetic current sensor accuracy and safety to EV powertrain applications," says Shaun Milano, Business Unit Director for current sensors at Allegro.

www.allegromicro.com


CDE
CORNELL DUBILIER
ENERGIZING IDEAS
IF IT'S NOT THE HEAT,
~AC
ALH SERIES
DC
BLH SERIES
IT'S THE HUMIDITY
Meet the 1,500-hour THB-rated ALH/BLH capacitors
At 85°C and 85% relative humidity, with rated voltage applied, our new inverter-grade film capacitors are tested 50% longer than the industry standard requirements for Temperature-Humidity-Bias. Improve the reliability of your power electronics design with outstanding capacitor performance at high humidity.
cde.com/harsh-environments
1,500 HOURS
85°C
85% RH
AEC-Q200

Consumer Drives Applications – Energy Efficiency and Power Density with SiC Power Devices

Over the past decades, energy regulations have been consolidated highlighting the importance of manufacturing energy efficient products. This has led to saving considerable amounts of energy [1]. Additionally, these directives have paved the way for designing more innovative appliances by utilizing new technologies such as SiC MOSFETs due to their superior intrinsic properties [2]. Adopting such technologies helps manufacturers target the highest energy class label.

By Konstantinos Patmanidis, Stefano Ruzza, Claudio Villani, Infineon Technologies

Introduction

Recently, a newly developed advanced integrated power device (IPD), IM105-M6Q1B, was introduced. IM105-M6Q1B offers the benefits of Infineon's CoolSiC™ technology and an industry benchmarked, high-voltage, rugged-driver integrated circuit (IC) in a small 7 mm x 7 mm quad flat no-lead (QFN) package. Using this IPD enables the designing of low power drives with superior power density as well as extending the output power limits of heat sink-less operation.

A test vehicle drive board was designed, as shown in figure 1, to test the capabilities of IM105-M6Q1B under typical fridge compressor loading conditions. The block diagram of IM105-M6Q1B is also included in the image. The IPD is composed of a SiC MOSFET half-bridge with a typical on-state resistance of 257 mΩ at V_{gs} = 18 V and T_j = 25°C, and a gate driver based on the silicon-on-insulator (SOI) technology. The maximum blocking voltage has been upgraded to 650 V compared to 600 V in standard devices, offering an additional margin in case of grid voltage fluctuations. Advantages of Infineon's SOI technology in gate drivers are high switching frequency functionality [3], low ohmic (30 Ω) monolithically integrated bootstrap diode [3, 4], and robust negative transient immunity due to inductive load switching events [5]. Additionally, this gate driver provides fixed internal dead time, typically of 540 ns, which is automatically inserted whenever the external dead time is shorter to ensure shoot-through protection. All these gate driver features, together with Infineon's CoolSiC™ technology advantages are offered in a small surface mounted device (SMD) package.

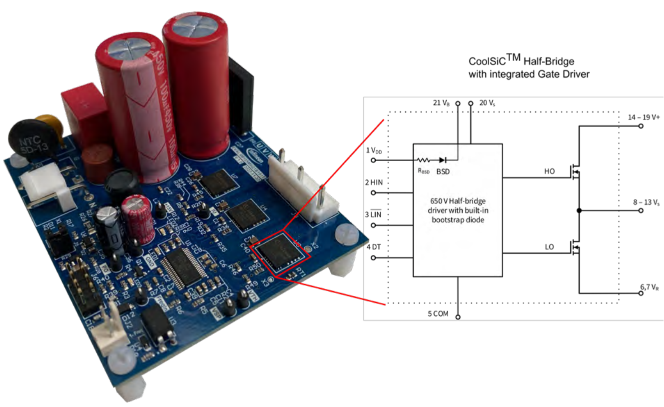

Figure 1: Drive board test vehicle and block diagram of IM105-M6Q1B.

On-state output characteristics

In this section, typical output characteristics of IM105-M6Q1B are discussed at two gate-biased voltages – 15 V and 18 V. In low power consumer drives market, two commonly employed products are IKD04N60RC2 and IPD60R280PFD7S. In this section, their output characteristics have also been compared with that of IM105-M6Q1B.

The first output characteristic graph is shown in figure 2. It can be seen that in the first quadrant operation, the voltage drop of IM105-M6Q1B is significantly lower (about 4 A) than that of IKD04N60RC2.

Moreover, the temperature dependency of IM105-M6Q1B on its $R_{DS(on)}$ is, typically, just 0.11 mΩ/°C at V_{gs} = 15 V and slightly higher, which is 0.2 mΩ/°C, at V_{gs} = 18 V. This highlights the minor temperature dependency characteristics of the CoolSiC™ technology. On the other hand, in the third quadrant operation during the conduction time interval of the diode, the voltage drop is higher for IM105-M6Q1B than for IKD04N60RC2. However, note that the diode only conducts during the dead time, which is roughly between 0.5 and 1 µs under application conditions, and therefore, its loss contribution is insignificant. When the SiC MOSFET channel conducts in the third quadrant operation, the voltage drop is slightly lower than the one in the first quadrant operation.

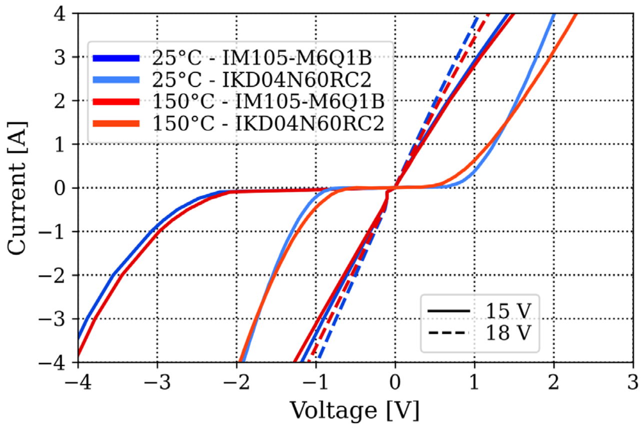

Figure 2: On-state output characteristics of IM105-M6Q1B against IKD04N60RC2

The second comparison graph is shown in figure 3. It is evident that the voltage drop of IPD60R280PFD7S in the first quadrant operation at T_j = 25°C is lower than that of IM105-M6Q1B. The typical $R_{DS(on)}$ of IPD60R280PFD7S is 233 mΩ at V_{gs} = 10 V and T_j = 25°C. For this device type, the increase of the gate bias does not provide additional reduction in voltage drop, as can be seen in its datasheet. Apart from this, it can be also be discerned that the voltage drop temperature dependency of IPD60R280PFD7S is significantly higher than that of IM105-M6Q1B. The typical $R_{DS(on)}$ temperature dependency of IPD60R280PFD7S is approximately 2.53 mΩ/°C,


Johannes Soldan, Stefanie Hagemann, Daniel Rückert, Steffen Knapp, GVA experts for development
gva-power.de
„WE ARE THE POWER-UP FOR YOUR IDEAS: GVA"
Our experts in the field of development belong to the "GENERATION INNOVATION". They develop innovative solutions from your ideas for IGBT and IGCT converters, medium voltage switches, switches in the kA range, surge current switches, rectifiers, soft starters and much more. What are you waiting for?
Your GVA expert:
Jürgen Kolasinski
+49 (0)621 / 78992-22
j.kolasinski@gva-power.de
GVA
POWER ELECTRONICS EXPERTS
in
YouTube

and thus higher conduction losses at elevated junction temperatures than IM105-M6Q1B are expected. Likewise, IPD60R280PFD7S exhibits a lower voltage drop for the forward-biased diode than IM105-M6Q1B.

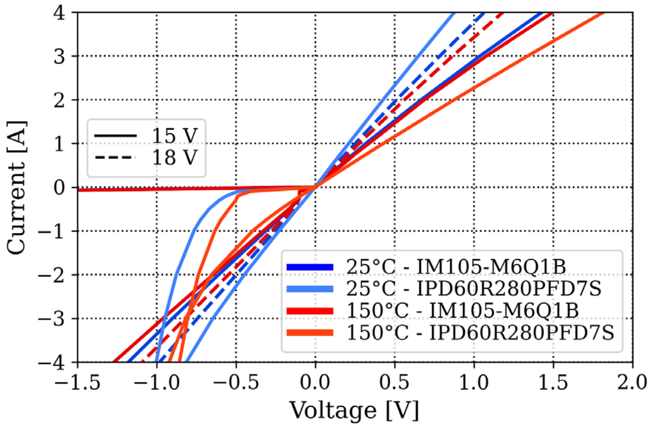

Figure 3: On-state output characteristics of IM105-M6Q1B against IPD60R280PFD7S.

Finally, the total typical dynamic losses of the aforementioned devices are shown in figure 4, as derived using a typical double-pulse test setup. Please note that reverse recovery losses were excluded from this analysis because their contribution to the total sum is relatively minor. The voltage rate of change, dv/dt, for both the devices was tuned to be similar at roughly 6.5 – 7 V/ns, to ensure a fair comparison. The switching speed of IM105-M6Q1B was tuned internally by its integrated gate driver to be between 6 and 7 V/ns (20 – 80%).

IM105-M6Q1B shows significantly lower energy losses when compared to IKD04N60RC2 and particularly IPD60R280PFD7S, the energy losses of which are dominated by turn-on losses. Last but not least, the dynamic losses of IM105-M6Q1B present negligible dependency on temperature, while in other devices, even at T_j = 100°C, the losses start increasing considerably.

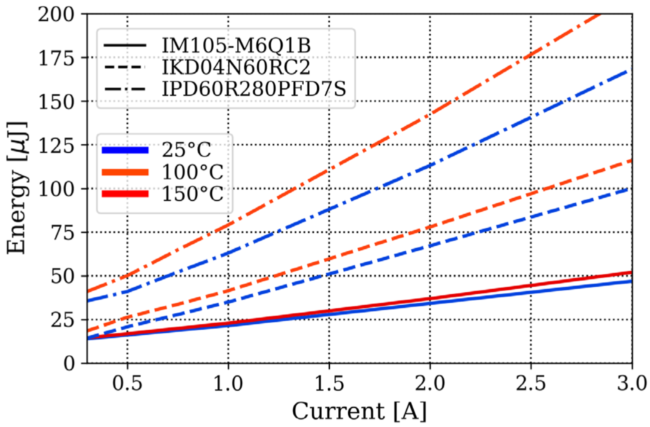

Figure 4: Sum of the turn-on and turn-off dynamic losses at different switching currents and temperatures.

Typical fridge compressor simulation analysis

A typical fridge compressor presents several operating points throughout its total cycle. The two most distinctive ones are the rated operating point at which the output power is about 40 W, and the high load operation in which the output power is roughly 160 W. In this analysis, the PLECS® software tool was used to examine the power losses of the three case study devices. The outcome of the simulation together with typical application conditions is shown in figure 5 and figure 6. The case temperature for these simulations was set to T_c = 110°C. This is, typically, the maximum operating case temperature of a printed circuit board (PCB), as it is limited due to its material properties. At light load or the rated load, IM105-M6Q1B showed almost 43 percent lower losses than IPD60R280PFD7S and 60 percent lower losses than IKD04N60RC2. Under these conditions, increasing the gate voltage to V_{gs} = 18 V did not provide noticeable benefits.

In the case of high load, IM105-M6Q1B showed almost 37 percent lower losses than IPD60R280PFD7S and 64 percent lower losses than IKD04N60RC2. Here, increasing the gate voltage of IM105-M6Q1B to V_{gs} = 18 V offered relatively 14 percent lower losses than with the gate voltage V_{gs} = 15 V, indicating the minimum achievable losses of IM105-M6Q1B.

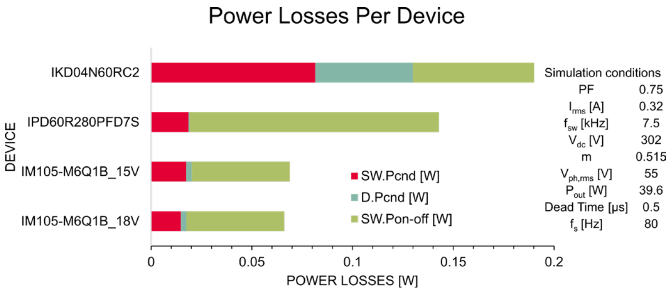

Figure 5: Split graph of power losses of a typical fridge compressor at given rated conditions.

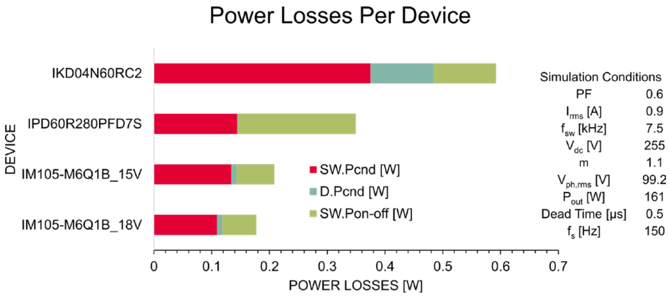

Figure 6: Split graph of power losses of a typical fridge compressor at given high load conditions.

The efficiency calculation for the inverter stage is given in table 1. A 2-level, 3-phase inverter was considered in this analysis, i.e., six devices in total. At nominal load, the overall efficiency gain of IM105-M6Q1B was 2.7 percent more than IKD04N60RC2 and almost 1 percent more than IPD60R280PFD7S. At high load conditions, the efficiency gain was roughly 1.5 percent and 0.5 percent against IKD04N60RC2 and IPD60R280PFD7S respectively.

Device	**Efficiency [%]**	
	Nominal load	High load
IM105-M6Q1B_18 V	98.77	99.29
IM105-M6Q1B_15 V	98.74	99.17
IPD60R280PFD7S	97.82	98.69
IKD04N60RC2	96.95	97.75

Table 1: Efficiency calculation of a 6-bridge, 2-level, 3-phase inverter

Hardware experiment results

This section discusses additional benefits of IM105-M6Q1B in terms of form factor, i.e., power density. A comparative analysis of the heat sink-less output power capability of similarly designed low power drive boards with IKD04N60RC2 and IM105-M6Q1B is also provided. Images of the drive boards are shown side by side in figure 7, to clearly highlight their differences. Both boards include similar electromagnetic interference (EMI) filters, diode rectifiers, DC link capacitors, and the microcontroller IMC101T-T038 (iMOTION™ IMC100 motor controller).

Both designs have a layout with two copper layers and 35 µm copper traces thickness. The main difference lies at the inverter stage.

Immerse yourself in our exciting world of industrial automation

Get a detailed overview of Infineon's industrial automation product and solution portfolio with our new interactive graphic

Infineon has extensive expertise in efficient automation and drive solutions for the various levels of an industrial smart factory. Explore our high-quality, industrial-grade semiconductors, along with a range of proven reference designs for your next automation design.

Explore here :
www.infineon.com/automation

The drive board using IKD04N60RC2 requires six discrete IGBTs in a TO-252 package and one full-bridge, 3-phase gate driver IC to form a two-level, 3-phase inverter. On the other hand, the board using IM105-M6Q1B requires significantly less space due to the integration of the half-bridge and gate driver into a QFN package. Consequently, the size of this board can be reduced by 15%, resulting in improved power density.

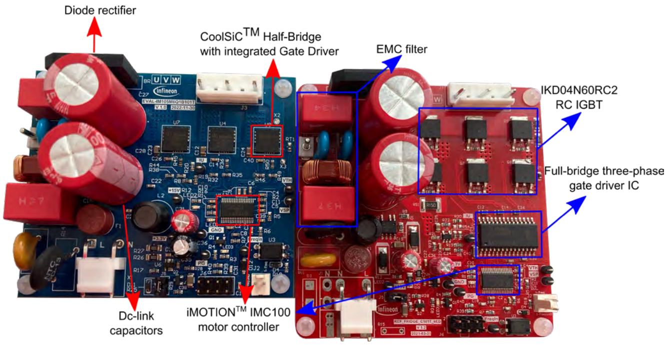

Figure 7: Low power consumer drives: The blue PCB (left side) uses IM105-M6Q1B, dimensions: 66.4 mm x 78 mm; the red PCB (right side) uses IKD04N60RC2, dimensions: 78 mm x 78 mm.

Low power consumer drives applications (e.g., fridge compressor, circulation pumps, and so on) typically have switching frequencies (f_{sw}) between 7.5 and 17 kHz. These applications are mainly heat sink-less because their low output power ensures that the power switches operate within their specified thermal limits. Their maximum allowable case temperature ($T_{c,max}$) is limited roughly to 110°C, as mentioned earlier.

To examine and analyze the performance of the drives under test conditions, a typical fridge compressor was chosen. Figure 8 shows the laboratory test bench with a fridge compressor as the load. A thermal camera was used to monitor the top side case temperature of the inverter. The control scheme was implemented using Infineon's iMOTION™ IMC101T-T038 microcontroller together with an isolated debug probe iMOTION™ Link. The drive under test was directly supplied to the DC link to avoid any grid voltage variations or loading effects on the voltage, and to enable the use of standard passive probes without requiring a floating measuring equipment. Passive probes were connected to the low side power devices to measure the typical dv/dt behavior of the devices. Finally, a current probe was connected in the output phase to monitor the motor's current.

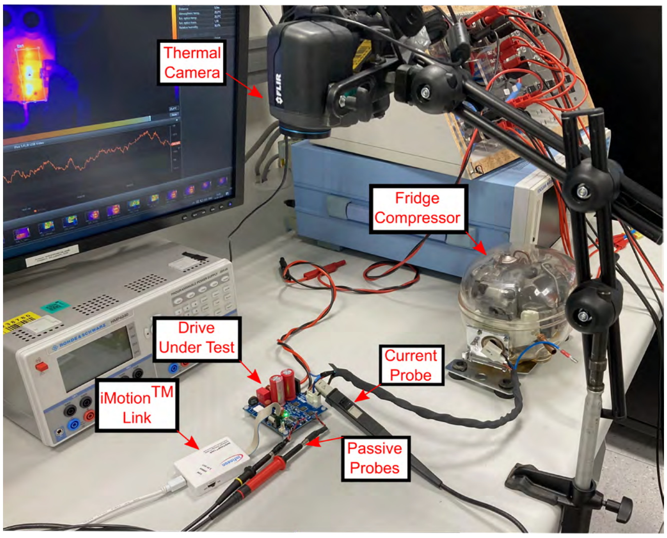

Figure 8: Laboratory test bench.

Two modulation techniques were applied—one space vector pulse-width modulation (SVPWM) with seven steps and one with five steps (offering reduced switching losses), as discussed in [6]. The experimental test conditions are listed in table 2. The DC link voltage was preset to 310 V for all experimental conditions, provided by a high voltage DC power supply unit. The output fundamental frequency (f_s) for the fridge compressor was configured to 20 Hz. The ambient temperature (T_a) was room temperature at roughly 25°C. The power factor (PF) was not measured to avoid any influence of additional parasitics. The only independent experiment variable was the modulation amplitude index. The modulation amplitude index was adjusted till the maximum case temperature, in the vicinity of the inverter, was reached, resulting in different allowable phase currents. This was realized using an open loop control scheme, in this case the V/f control because the focus was merely on the inverter stage. These experiments provide an indication to the board's maximum output power capability.

V_{dc} [V]	310
f_s [Hz]	20
T_a [°C]	25
f_{sw} [kHz]	7.5–17
V_{gs}–V_{ge} [V]	0–15, 18.5
$T_{c,max}$ [°C]	110
Dead time [µs]	1

Table 2: Experimental test conditions

The output power capability is shown in figure 9. For this graph, the output power was calculated considering a PF of 0.75 and modulation amplitude index of one. It is evident that IM105-M6Q1B is capable of delivering almost two times more power than the IKD04N60RC2 drive board, demonstrating also the improvements in power density. In this case study, the additional benefit of increasing the gate voltage to about V_{gs} = 18.5 V provided an additional 6% more output power than the case study with V_{gs} = 15 V.

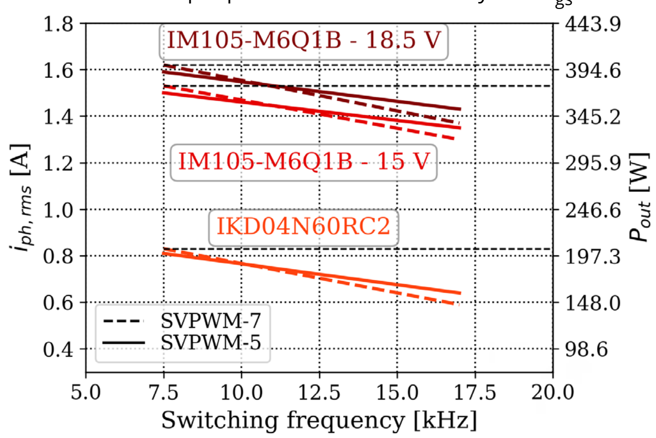

Figure 9: Maximum allowable phase current under different switching frequencies and modulation schemes.

Finally, the typical dv/dt behavior of the two devices used for this case study is shown in figure 10 and figure 11. The high side switch is denoted with HS and the low side with LS. Note that the turn-on dv/dt of IKD04N60RC2 was tuned to be about 6 to 7 V/ns.

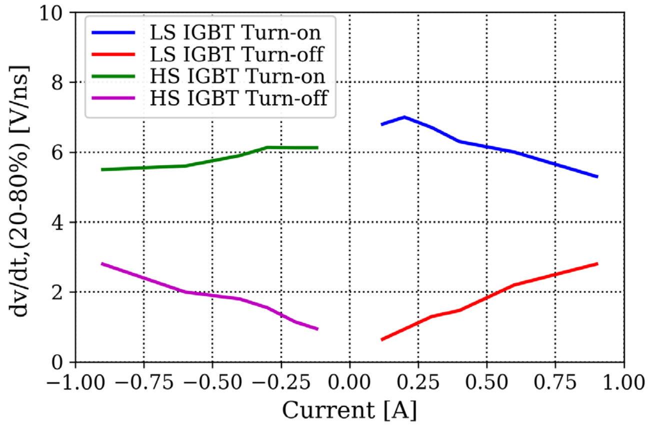

Figure 10: Voltage rate of change (dv/dt, 20 - 80%) at different switching currents at $T_{c,max}$ for the IKD04N60RC2 drive board tuned to 6.5 V/ns.

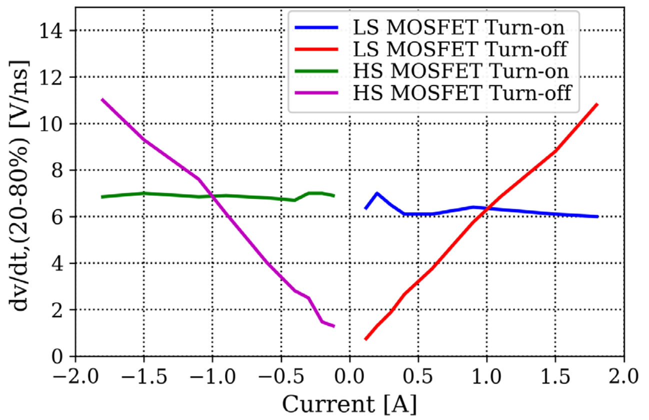

Figure 11: Voltage rate of change (dv/dt, 20 - 80%) at different switching currents at $T_{c,max}$ for the IM105-M6Q1B drive.

Conclusion

The newly introduced energy label directives for low power consumer drives applications, namely home appliances, emphasize the importance of developing innovative solutions and adopting new semiconductor technologies to reach the top level in the energy labeling scale. This article presented several benefits of Infineon's CoolSiC™ MOSFETs in an integrated product IM105-M6Q1B.

The small size of the QFN package, only 7 mm x 7 mm, helps design system level solutions with enhanced power density.

This was highlighted by designing a drive board with IM105-M6Q1B, which was 15% smaller in size than the discrete solution with IKD04N60RC2. IM105-M6Q1B also provides superior output power handling capability than IKD04N60RC2. Additionally, with the use of IM105-M6Q1B, inverter efficiency can be improved by 1 – 2.7%.

References

[1] A. C. Russo, M. Rossi, M. Germani, and C. Favi, "Energy label directive: Current limitations and guidelines for the improvement", Procedia CIRP, vol. 69, pp. 674–679, 2018, 25th CIRP Life Cycle Engineering (LCE) Conference, 30 April – 2 May 2018, Copenhagen, Denmark. doi: https://doi.org/10.1016/j.procir.2017.11.136.

[2] J. Millán, P. Godignon, X. Perpiñà, A. Pérez-Tomás, and J. Rebollo, "A Survey of Wide Bandgap Power Semiconductor Devices", in IEEE Transactions on Power Electronics, vol. 29, no. 5, pp. 2155–2163, May 2014, doi: 10.1109/TPEL.2013.2268900.

[3] J. Song, "Level-Shifter Current Influence to Power Loss of Gate Driver IC", PCIM Europe 2019; International Exhibition and Conference for Power Electronics, Intelligent Motion, Renewable Energy and Energy Management, Nuremberg, Germany, 2019, pp. 1–4.

[4] Frank, Wolfgang & Hellmund, Oliver & Boguszewicz, Viktor, "Compact and Powerful 600V Half Bridge Driver ICs for Consumer Electronics and Home Appliances", Bodo's Power Systems. 22. 2013.

[5] J. Song and W. Frank, "Robustness of level shifter gate driver ICs concerning negative voltages", PCIM Europe 2015; International Exhibition and Conference for Power Electronics, Intelligent Motion, Renewable Energy and Energy Management, Nuremberg, Germany, 2015, pp. 1–7.

[6] E. R. C. da Silva, E. C. dos Santos, and B. Jacobina, "Pulse-width Modulation Strategies," in IEEE Industrial Electronics Magazine, vol. 5, no. 2, pp. 37–45, June 2011, doi: 10.1109/MIE.2011.941120.

www.infineon.com

Power Modules in Embedded Drives

While embedded motor drives are gaining popularity in industrial applications, their compact size and tight integration present new challenges in terms of heat dissipation and electromagnetic interference. This article outlines these challenges and presents how they can be overcome using Vincotech thickfilm technology.

By Patrick Baginski, Vincotech GmbH, Unterhaching/Germany

Motor drive applications are considered state of the art in many industrial businesses. Most standard induction motors operate from fixed frequency sinusoidal power. These days, however, motors with adjustable or variable frequency drives (VFDs) are gaining popularity. These can be broken down into two categories: The first, decentralized drives, use an external inverter mounted, for example, on the motor connection box. Embedded drives, on the other hand, use an internal inverter that is part of the motor itself and can sometimes not even be seen from outside.

The main design constraints for embedded drives used, for example, in non-industrial fans and pumps, are space availability and the reduction of motor and inverter losses. In addition, they need to fulfill power factor requirements.

Environmental conditions

Moving the inverter from the control cabinet to the motor has led to new inverter design requirements. Among the most demanding is thermal management. Standard cabinet-mounted inverters operate in a rather friendly environment with no particular IP protection requirements, unlike the motor, which is installed somewhere in the production line near the goods that are being processed. By contrast, embedded drives use an internal inverter, which requires both the motor and the inverter to be water- and dustproof, impacting the system's thermal properties.

In IP65 protected systems, the dissipated power of all components can only exit through their surface, mainly via the heatsink. Inverters used in embedded systems must, therefore, be designed to minimize power dissipation and to connect all their power dissipating components to the heat sink using a good thermal interface. By keeping the overall temperature low and avoiding hot spots inside the system, this ensures overall system reliability.

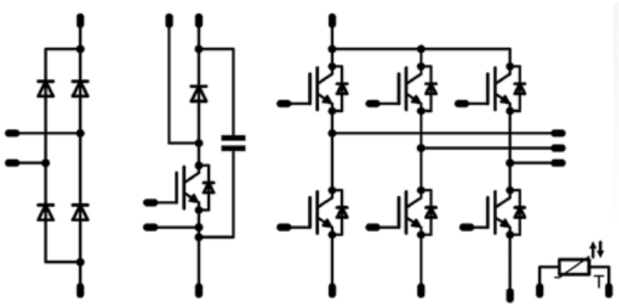

Figure 1: CI + PFC topology

In addition, inverters have to be small enough to fit into a given environment to enable a compact motor design and high installation density. Examples can be found in the water treatment, heat pumps, and ventilation systems. The reduction of the system's surface area makes optimized thermal management even more important. At the same time, shrinking overall system volume requires an intelligent system split that minimizes interconnections between the power section, the energy storage, and the inverter's control board.

Common requirements across all applications are rectifier diodes, a passive or active PFC, and an inverter stage for the motor as shown in Figure 1. An additional PFC circuit is required to fulfill the Energy Efficiency Directive, established in 2012 to develop applications with higher efficiency.

Figure 2 shows two well-known applications of embedded drives that illustrate the compactness enabled by integrated inverters.

Figure 2: A Wilo pump and an ebm-papst fan as examples of embedded drive systems

The challenge lies in moving components with creepage and clearance requirements – that need a lot of space on the PCB – to new locations where other rules apply. These components include the CI + PFC semiconductors as well as parts for the boot-strap circuit, shunts, snubber capacitors, etc. And this is where the power module comes into play. Power modules are usually filled with an electrically isolating silicone gel with a dielectric strength of several kilovolts per millimeter. Covering components with silicone makes it possible to pack them more densely.

One obstacle is the minimum distance between two tracks, which needs to be >0.5 mm when a standard Al2O3 DCB is used. This is less of an issue for bare dies of power semiconductors but becomes more challenging for discrete components such as resistors, capacitors, and diodes, and even more so for ICs. In these cases, Vincotech's thickfilm technology offers the most promising solutions, with achievable fine pitch distances of less than 0.5 mm.

Vincotech offers two types of modules for embedded drive applications: DCB modules that only include power semiconductors, and thickfilm modules that also include active and passive components. While both are based on aluminum oxide, their main differences are the base material thickness and whether they have copper planes on either side. Because Al2O3 is a fragile material and needs to be handled with care, thickfilm substrates are about twice as thick as DCBs, at about 1 mm. Additionally, they have a higher thermal resistance because the absence of the top and bottom copper does not allow thermal spreading.

Thickfilm modules are based on a technology that allows to print different layers on an aluminum oxide substrate, which is then fired at 850 °C. A variety of pastes are available for different purposes, such as low ohmic conductors for high power tracks and resistor pastes ranging from low values for shunts to high values in the MΩ range for all kinds of resistor functions.

Laser trimming the resistors increases their accuracy and adding a glass passivation layer improves their reliability.

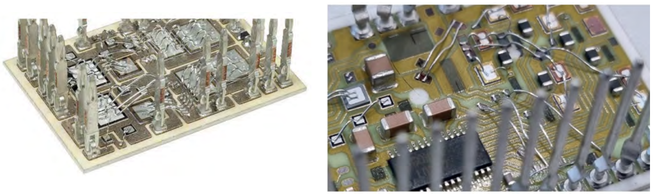

Figure 3: Comparing a DCB-based module (left) and a thickfilm module (right)

The schematic below depicts the components that are integrated into the thickfilm module. First, unlike in the case of standard power modules, the gate driver IC is implemented including diodes, resistors and – this is very rare –capacitors. Finally, it shows a gate resistor and a gate-emitter capacitance as an example. Other Vincotech thickfilm products have different turn-on and turn-off gate resistors and, optionally, a gate-emitter resistance to discharge the gate in the absence of a power supply.

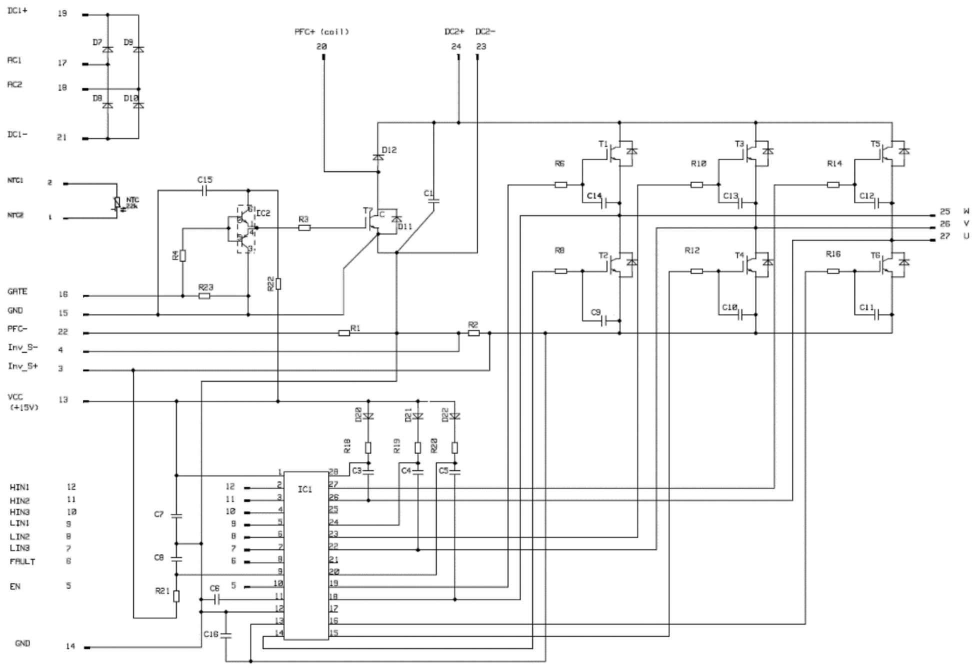

Figure 4: Internal circuit of a thickfilm power module

The circuit also includes a PFC circuit with a fast 650 V IGBT or an even faster Si MosFet as well as a fast Si diode or, when even higher switching frequencies and efficiencies are required, a SiC diode.

A ceramic capacitor between DC+ and DC- closes the high frequency loop inside the power circuit. Capacitors between the gate and the emitter further improve EMI as shown in Figure 5.

Capacitor placement can strongly impact measured values.

Summary

Two different types of power modules are widely used in embedded drive applications: DCB modules that only include power semiconductors like a PFC stage and the inverter stage, and highly integrated modules based on thickfilm technology. Vincotech IPMs based on thickfilm technology make it possible to add passive components where they are needed: as closely as possible to the power semiconductors. Components such as the complete boot strap circuit, which includes capacitors and shunt resistors, offer engineers clear benefits in terms of size. Moreover, they can design PCBs without having to add additional creepage and clearance distances, making it possible to further shrink their applications. The outstanding electrical properties of other components, such as the X2 and gate emitter capacitors, make it possible to reduce the size of some of the filters on the PCB and, in some cases, even making them obsolete.

Vincotech's modules for embedded drive systems and thickfilm based products are the perfect solution for higher system integration and higher power densities.

www.vincotech.com/EmbeddedDrives

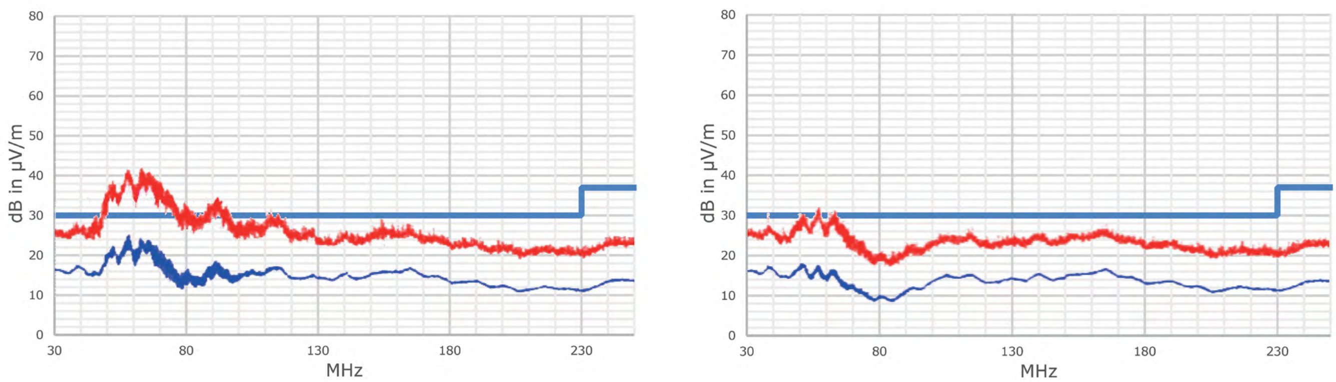

Figure 5: EMI measurement without Cge (left) and with integrated Cge (right)

Easy to Use and Compact: A Family of SiC Power Modules for Automotive Traction Inverters

eMobility is rapidly gaining market share, resulting in a growing need for power electronics such as inverters. Some of the power electronics manufacturers optimize their power modules by replacing the Si IGBTs through the SiC MOSFETs in the high-volume mainstream packages. However, it is not sufficient to just replace the semiconductors. It is necessary to develop and optimize new packages which are adjusted to the SiC demands.

By Yevgeniy Temko, Philipp Mueller, Anne Bedacht*
**corresponding author, all Robert Bosch GmbH*

Over the last decade, Bosch has been driving electrification forward with customer-specific power modules based on IGBTs. In December 2021, Bosch introduced its first generation of SiC MOSFETs to the market. The 2nd Gen is currently in ramp-up phase, further reducing conduction and switching losses and allowing for even higher switching frequencies.

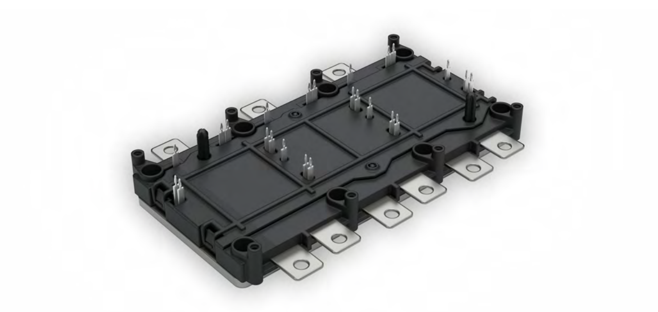

Figure 1: CSL B6 bridge with screw contacts (top view)

Combining these two areas of expertise, Bosch now presents the CSL (Compact Silicon Carbide Line) power module family for traction inverters. The CSL family is scalable for power ratings from 75 kW to 250 kW – more than 50% of the traditional ICE passenger vehicle fleet[1] falls in this range.

In comparison to commercially available gel frame solutions, CSL modules are smaller in size, allowing for cost-effective inverter designs. MOSFETs with breakdown voltages of 750 V and 1,200 V make them the ideal choice for 400 V or 800 V inverter systems.

The module DC busbars and phase contacts can be connected to the DC Link / battery / EMC filter and e-machine busbars either via screwing tabs with holes (Figure 1) or via welding contacts (tabs integrated into module body) for high volume production (Figure 2). Despite the small form factor, CSL modules are still compatible with DC link capacitors for commercially available gel frame modules with screwable contacts.

Signal pins in press fit technology connect the frame module to the gate driver printed circuit board. The use of press fit contacts effectively avoids potential solder drips on the AMB. For highest contact reliability, the press fit pins are embedded in the frame mold material.

Two cooling options are available: an industrially common PinFin cooler or an integrated closed cooler[2] .

An uppermost performance of the adjoined materials such as gel, frame, AMB with Si3N4 isolation, baseplate, double-sided sintering of the SiC die with die top system Cu termination and Cu thick wire bonding allows operation at a steady state temperature of 175°C.

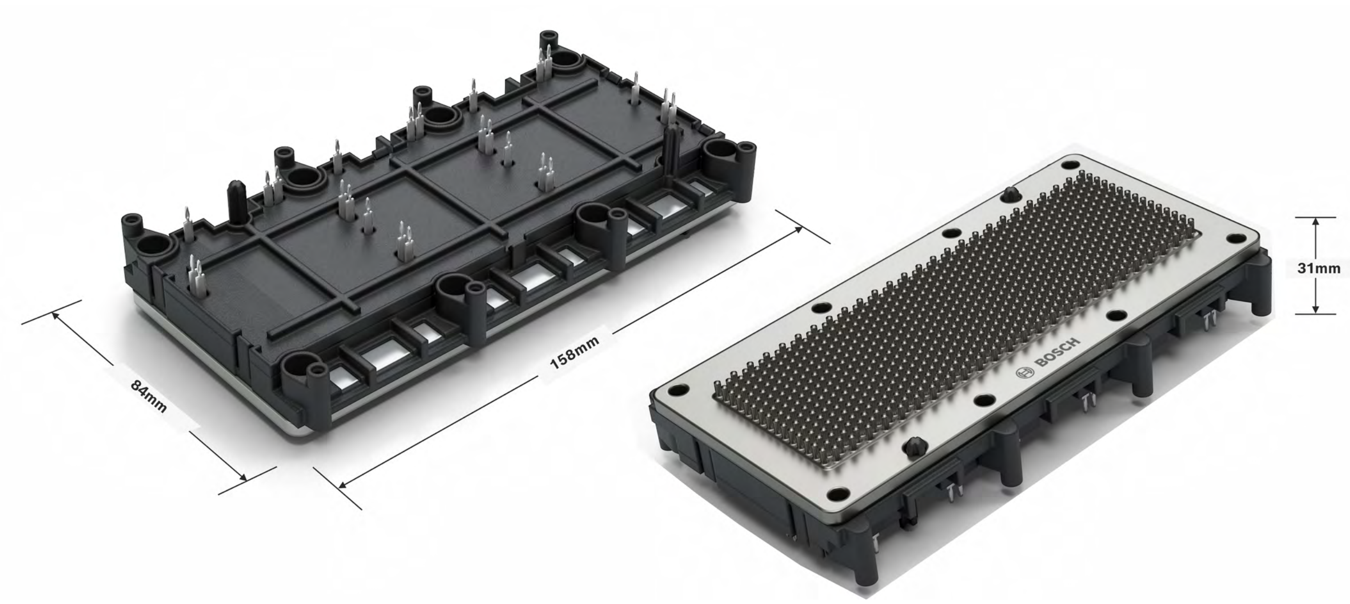

Figure 2: CSL B6 bridge, weld version (top and bottom view)

For efficient cooling, the module features an optimized thermal path. The SiC MOSFETs are sintered on a Si_3N_4 AMB, the AMB is soldered on the cooler for lowest thermal resistance R_{th}.

To exploit the full potential of the MOSFETs, special attention was paid to a symmetrical layout and to the placement of the SiC MOSFETs.

Every phase incorporates a separate NTC for MOSFET temperature measurement. For accurate temperature reading, the NTCs are located in the high side path, as close as possible to the MOSFET dies.

The CSL complies with AQG 324 and is RoHS compatible, all plastic components are UL94 V-0 compliant and therefore flame-retardant.

The compact design also contributes to reduced leakage inductances, enabling high switching dynamics. For the screw variant, the internal stray inductance is typically less than 10 nH. For the weld variant, internal stray inductance is typically less than 6 nH.

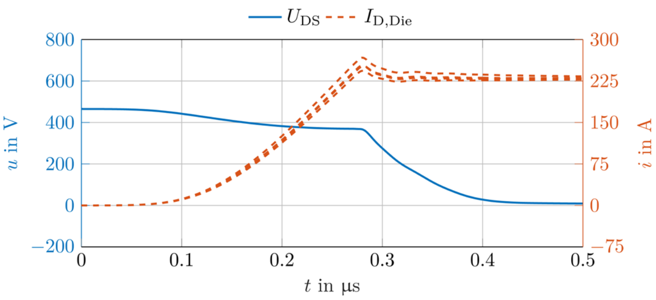

Figure 3: Dynamic Switching of 750 V CSL module at Tj =175 °C and 920 A

With outline dimensions of 158 x 84 x 31 mm (see Figure 2), the weld version is 35% smaller in volume than other commercially available frame modules for automotive traction inverters.

In addition, the high dynamics of the weld variant enables efficient partial load operation. The efficiency is further increased by fast transients and low R_{DSon}.

Figure 3 shows the current waveform of four MOSFETs switched in parallel. The start junction temperature in this operation point is 175 °C at 920 A. The current mismatch between the MOSFETs is 5 % max.

The low mismatch leads to an optimal utilization of the SiC MOSFETs. Ringing between the MOSFETs is minimized, asymmetrical stress and aging is reduced. The symmetrical current distribution also results in an improved short-circuit robustness.

Short-circuit capability is further increased by a current feedback, helping to reduce the peak short-circuit current $\hat{I}_{SC}$.

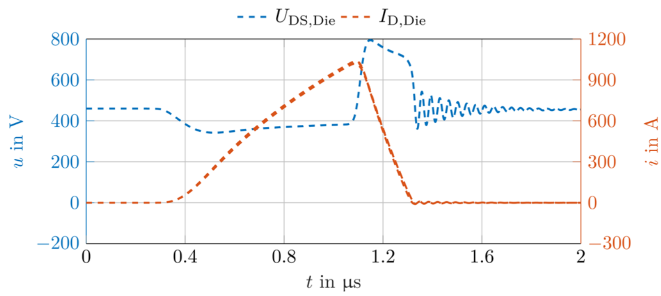

Figure 4: Short-circuit type 1 of 750 V CSL module at Tj =175 °C and 460 V

Figure 4 shows the current waveform for a short-circuit type 1. The start temperature of the event is 175 °C with an applied DC link voltage of 460 V.

The interaction of layout and chip design increases the critical short-circuit time, while at the same time RDSon is kept low at typically 1.4 mΩ.

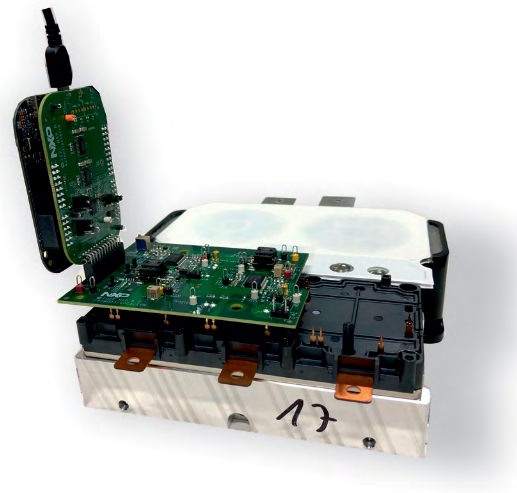

Figure 5: FRDMGD3160CSLEVM half-bridge evaluation kit from NXP for dynamical measurements on CSL modules For more information, visit NXP's website (https://nxp.com/FRDMGD3160CSLEVM)

The selected interconnection technology enables high pulse loads during operation and a high current carrying capacity - even at high temperatures in the safe state of the traction inverter.

For a comfortable validation of the module's performance and capabilities, Bosch collaborated with NXP Semiconductors to develop a custom gate driver evaluation board, using advanced high-voltage isolated gate drivers (GD3160). The result is the FRDMGD3160CSLEVM, a half-bridge evaluation kit, implemented using two GD3160 ICs, a KL25Z microcontroller to interface to a PC, and free FlexGUI interface software. The software allows users to perform dynamic SiC switching measurements (e.g., double pulse and short-circuit type 1,2 tests) on all CSL module B2 bridges. Figure 5 shows the evaluation board attached to the module.

Summary

The CSL (Compact SiC Line) B6 bridge family addresses the requirements of mainstream automotive traction inverters. Using the 2nd Gen of Bosch SiC MOSFETs allows for lowest switching and conduction losses and a smooth dynamic behavior. With its symmetrical AMB design, the CSL family provides high performance during normal and special operating conditions.

References

1. Exawatt, Silicon Carbide in Electric Vehicles: Market Outlook, Edition of July 2022.
2. Bosch Website: https://www.bosch-semiconductors.com/power-semiconductors/

www.bosch.com

How to Optimize Switching Power Supply Layout by Minimizing Hot Loop PCB ESRs and ESLs

For power converters, a hot loop PCB layout with minimum parasitic parameters can improve the power efficiency, lower the voltage ringing, and reduce the electromagnetic interference (EMI). This article discusses the optimization of hot loop layout design by minimizing the PCB equivalent series resistances (ESRs) and equivalent series inductances (ESLs).

By Jingjing Sun, Product Applications Senior Engineer, Ling Jiang, Product Applications Manager, and Henry Zhang, Product Applications Senior Director; Analog Devices

This article investigates and compares impact factors including decoupling capacitor positions, power FET sizes and positions, and via placements. Experiments are conducted to verify the analysis, and effective methods of minimizing the PCB ESRs and ESLs are summarized.

Hot Loop and PCB Layout Parasitic Parameters

The hot loop of a switching-mode power converter is defined as the critical high frequency (HF) AC current loop formed by the HF capacitor and adjacent power FETs. It is the most critical part of the power stage PCB layout because it contains high dv/dt and di/dt noisy content. A poorly designed hot loop layout suffers from a high level of PCB parasitic parameters, including the ESL, ESR, and equivalent parallel capacitance (EPC), which have a significant impact on the power converter's efficiency, switching performance, and EMI performance.

Figure 1 shows a synchronous buck step-down DC-to-DC converter schematic. The hot loop is formed by MOSFETs M1 and M2 and the decoupling capacitor C_{IN}. The switching actions of M1 and M2 cause HF di/dt and dv/dt noise. C_{IN} provides a low impedance path to bypass the HF noisy content. However, parasitic impedance (ESRs, ESLs) exists within the components' packages and along the hot loop PCB traces. The high di/dt noise through ESLs causes HF ringing, furthermore, resulting in EMI. The energy stored in ESL is dissipated on ESRs, leading to extra power loss. Therefore, the hot loop PCB ESRs and ESLs should be minimized to reduce the HF ringing and improve efficiency.

An accurate extraction of the hot loop ESRs and ESLs helps predict the switching performance and improve the hot loop design. Both components' package and PCB traces contribute to the total loop parasitic parameters. This work mainly focuses on the PCB layout design. There are tools for users to extract the PCB parasitic parameters, such as Ansys Q3D, FastHenry/FastCap, StarRC, etc.

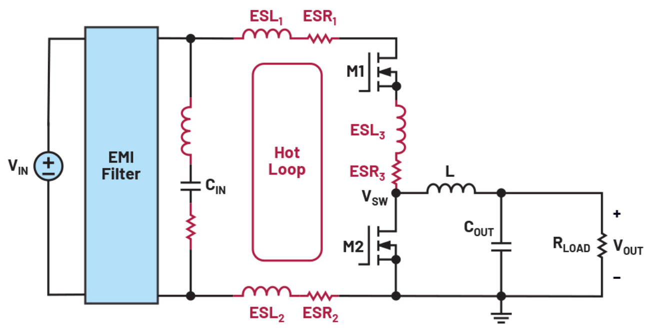

Figure 1: A buck converter with hot loop ESRs and ESLs.

Commercial tools like Ansys Q3D provide accurate simulation but are usually expensive. FastHenry/FastCap is a free tool based on partial element equivalent circuits (PEEC) numerical modeling[1] and can provide flexible simulation through programming to explore different layout designs, though additional coding is required. The effectiveness and accuracy of the parasitic parameter extraction in FastHenry/FastCap have been verified and compared to Ansys Q3D with consistent results.[2,3] In this article, FastHenry is used as a cost-efficient tool to extract PCB ESRs and ESLs.

Hot Loop PCB ESR and ESL vs. Decoupling Capacitor Position

In this section, the impacts of C_{IN} position are investigated based on ADI's LTM4638 µModule® regulator demo board DC2665A-B. The LTM4638 is an integrated 20 V_{IN}, 15 A step-down buck converter module in a tiny 6.25 mm × 6.25 mm × 5.02 mm BGA package. It offers high power density, fast transient response, and high efficiency. The module integrates a small HF ceramic C_{IN} inside, though it is not sufficient yet, limited by the module package size. Figures 2 to 4 illustrate three different hot loops on the demo board with additional external C_{IN}. The first one is the vertical Hot Loop 1 (Figure 2), where C_{IN1} is placed on the bottom layer just beneath the µModule regulator. The µModule V_{IN} and GND BGA pins are connected to C_{IN1} directly through the vias. These connections provide the shortest hot loop path on the demo board. The second hot loop is the vertical Hot Loop 2 (Figure 3), where C_{IN2} is still placed on the bottom layer, but moved to the side area of the µModule regulator. As a result, an extra PCB trace is added to the hot loop and larger ESL and ESR are expected compared to vertical Hot Loop 1. The third hot loop option is the horizontal hot loop (Figure 4), where C_{IN3} is placed on the top layer close to the µModule regulator. The µModule V_{IN} and GND pins are connected to C_{IN3} through the top layer copper without going through vias. Nevertheless, the V_{IN} copper width on the top layer is limited by the other pinout, resulting in an increased loop impedance compared to that of vertical Hot Loop 1. Table 1 compares the extracted PCB ESRs and ESLs of the hot loops by FastHenry. As expected, the vertical Hot Loop 1 has the lowest PCB ESR and ESL.

Hot Loop	ESR ($ESR_1 + ESR_2$) at 600 kHz (mΩ)	ESL ($ESL_1 + ESL_2$) at 200 MHz (nH)
Vertical Hot Loop 1	0.7	0.54
Vertical Hot Loop 2	2.5	1.17
Horizontal Hot Loop	3.3	0.84

Table 1: Extracted PCB ESRs and ESLs in Different Hot Loops by Using FastHenry

To experimentally verify the ESRs and ESLs in different hot loops, the demo board efficiency and V_{IN} AC ripple at 12 V to 1 V CCM operation are tested. Theoretically, a lower ESR leads to higher efficiency, and smaller ESL results in higher VSW ringing frequency and lower V_{IN} ripple magnitude. Figure 5a shows the measured efficiency. The vertical Hot Loop 1 gives the highest efficiency that corresponds to the lowest ESR. The loss difference between the horizontal hot loop and vertical Hot Loop 1 is also calculated based on the extracted ESRs, which is consistent with the testing result as shown in Figure 5b. The V_{IN} HF ripple waveforms in Figure 5c are tested crossing C_{IN}. The horizontal hot loop has a higher V_{IN} ripple magnitude and a lower ringing frequency, thus validating the higher loop ESL compared to the vertical Hot Loop 1. Also, because of the higher loop ESR, the V_{IN} ripple in the horizontal hot loop damps faster than in the vertical Hot Loop 1. Furthermore, a lower V_{IN} ripple reduces EMI and allows a smaller EMI filter size.

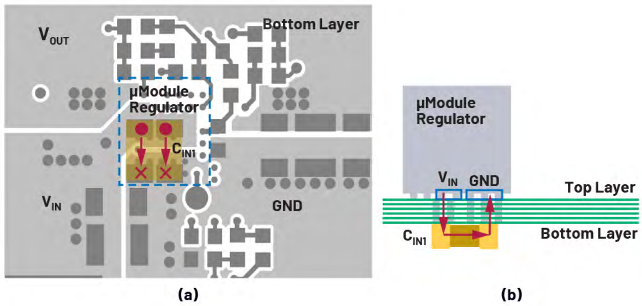

Figure 2: Vertical Hot Loop 1: (a) top view and (b) side view.

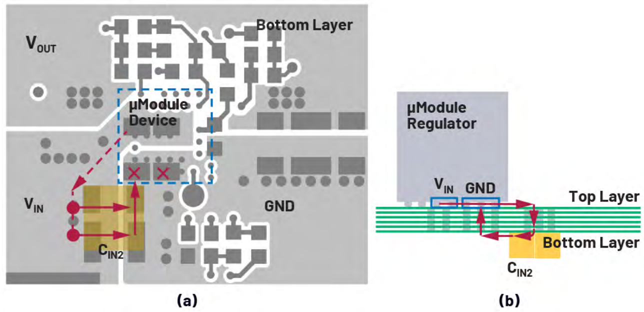

Figure 3: Vertical Hot Loop 2: (a) top view and (b) side view.

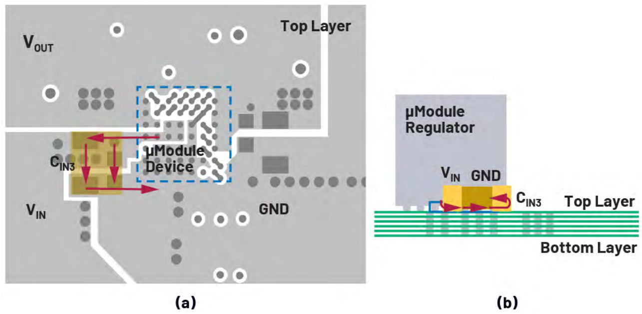

Figure 4: Horizontal hot loop: (a) top view and (b) side view.

Hot Loop PCB ESR and ESL vs. MOSFETs Size and Position

For a discrete design, the placement and package size of power FETs also have a significant impact on hot loop ESRs and ESLs. A typical half-bridge hot loop with power FETs M1 and M2 and a decoupling capacitor C_{IN} is modeled and investigated in this section. As illustrated in Figure 6, popular power FET package sizes and placement positions are compared. Table 2 shows the extracted ESRs and ESLs in each case.

Cases (a) to (c) present three popular power FET placements with 5 mm × 6 mm MOSFETs. The physical length of the hot loop determines the parasitic impedance. Hence, both 90˚ shape placement in Case (b) and 180˚ shape device placement in Case (c) result in 60% ESR reduction and 80% ESL reduction because of the shorter loop paths compared to those in Case (a). Since a 90˚ shape placement shows the benefit, several more cases are investigated based on Case (b) to further reduce the loop ESR and ESL. In Case (d), a 5 mm × 6 mm MOSFET is replaced with two 3.3 mm × 3.3 mm MOSFETs in parallel. The loop length is further shortened thanks to the smaller MOSFETs footprint, leading to 7% reduction of the loop impedance. In Case (e), when a ground layer is placed under the hot loop layer, the hot loop ESR and ESL are further decreased by 2% compared to Case (d). The reason is that eddy current is generated on the ground layer, which induces the opposite magnetic field and equivalently reduces the loop impedance. In Case (f), another hot loop layer is constructed as the bottom layer. If two paralleled MOSFETs are symmetrically placed on the top layer and bottom layer and connected through vias, the hot loop PCB ESR and ESL reduction are more obvious because of the paralleled impedance. Therefore, smaller sized devices with symmetrical 90˚ shape or 180˚ shape placement on top and bottom layers lead to the lowest PCB ESR and ESL.

To experimentally verify the impact of the MOSFETs placement, ADI's high efficiency, 4-switch synchronous buck-boost controller demo boards LT8390/DC2825A and LT8392/DC2626A are used.4 As shown in Figure 7a and Figure 7b, the DC2825A has a straight MOSFETs placement and the DC2626A has a 90˚ shape MOSFETs placement. To make a fair comparison, the two demo boards are configured with the same MOSFETs and decoupling capacitors, and tested at 36 V to 12 V/10 A, 300 kHz step-down operation. Figure 7c shows the tested V_{IN} AC ripple during M1 turn-on moment. With the 90˚ shape MOSFETs placement, the V_{IN} ripple has lower magnitude and higher resonant frequency, hence validat-

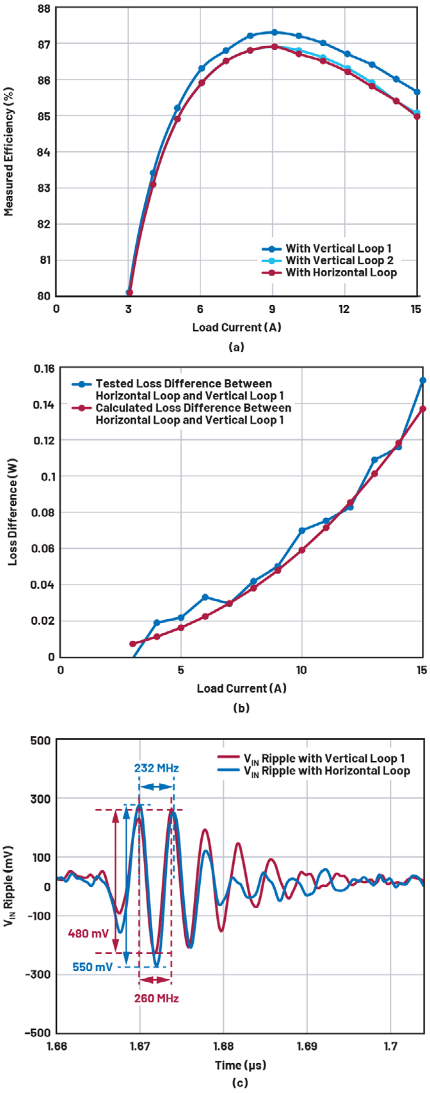

Figure 5: Demo board testing results: (a) efficiency, (b) loss difference between horizontal loop and vertical Loop 1, and (c) VIN ripple during M1 turn-on at 15 A output.

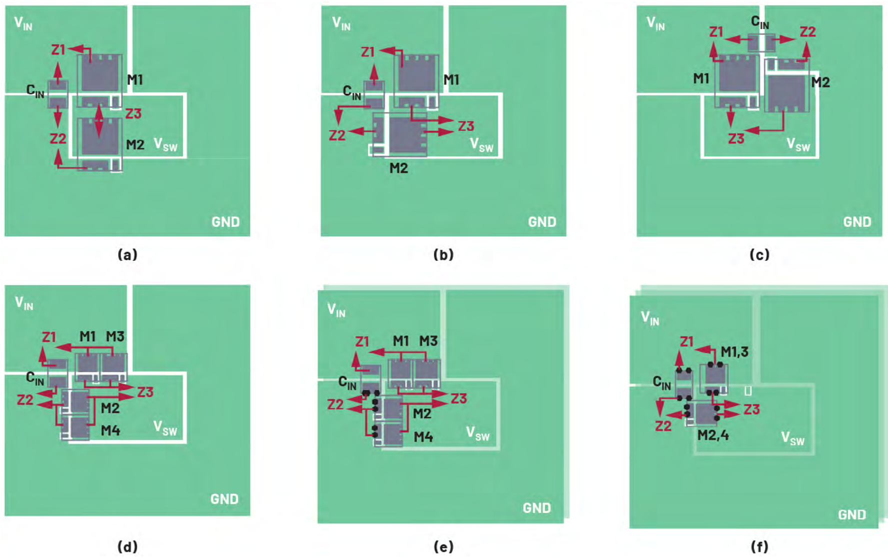

Figure 6: Hot loop PCB models: (a) 5 mm × 6 mm MOSFETs in straight placement; (b) 5 mm × 6 mm MOSFETs in 90˚ shape placement; (c) 5 mm × 6 mm MOSFETs in 180˚ shape placement; (d) two-parallel 3.3 mm × 3.3 mm MOSFETs in 90˚ shape placement; (e) two-parallel 3.3 mm × 3.3 mm MOSFETs in 90˚ shape placement with ground layer; (f) symmetrical 3.3 mm × 3.3 mm MOSFETs on top and bottom layers in 90˚ shape placement

	ESR_1 (mΩ) at 2 MHz	ESR_2 (mΩ) at 2 MHz	ESR_3 (mΩ) at 2 MHz	ESR_{TOTAL} (mΩ) at 2 MHz	ESR Change Rate vs. (a)	ESL_1 (nH) at 200 MHz	ESL_2 (nH) at 200 MHz	ESL_3 (nH) at 200 MHz	ESL_{TOTAL} (nH) at 200 MHz	ESL Change Rate vs. (a)
(a)	0.59	2.65	0.45	3.69	N/A	0.42	2.80	0.23	3.45	N/A
(b)	0.59	0.3	0.38	1.27	–66%	0.42	0.09	0.17	0.67	–81%
(c)	0.24	0.27	0.83	1.35	–63%	0.07	0.07	0.52	0.66	–81%
(d)	0.44	0.3	0.28	1.01	–73%	0.25	0.09	0.08	0.42	–88%
(e)	0.44	0.27	0.26	0.97	–74%	0.21	0.08	0.07	0.36	–90%
(f)	0.31	0.27	0.13	0.7	–81%	0.12	0.07	0.02	0.21	–94%

Table 2: Extracted Hot Loop PCB ESR and ESL with Various Device Shapes and Positions in FastHenry

ing the smaller PCB ESL due to a shorter hot loop path. On the contrary, because of the longer hot loop and higher ESL, the straight MOSFETs placement results in much higher V_{IN} ripple magnitude and slower resonant frequency. A higher input voltage ripple also causes a more severe EMI emission according to the EMI test results in the study of Cho and Szokusha.[4]

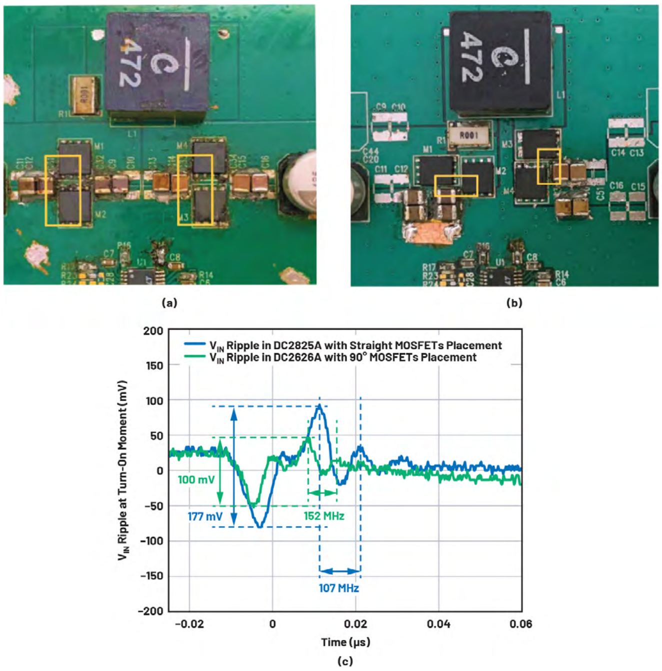

Figure 7: (a) LT8390/DC2825A hot loop with straight MOSFETs placement; (b) LT8392/DC2626A hot loop with 90˚ MOSFETs placement; (c) V_{IN} ripple waveforms at M1 turn-on.

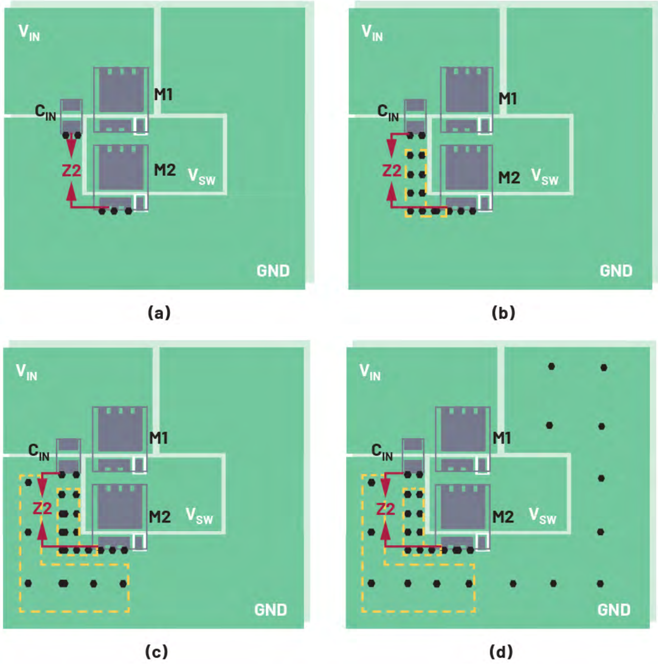

Figure 8: Hot loop PCB models with (a) five GND vias placed close to C_{IN} and M2; (b) 14 GND vias placed between CIN and M2; (c) 6 more vias placed on GND based on (b); (d) nine more vias placed on GND area based on (c).

Hot Loop PCB ESR and ESL vs. Via Placement

The vias placement in the hot loop also has a critical impact on the loop ESR and ESL. As shown in Figure 8, the hot loop with a two-layer PCB structure and straight power FETs placement is modeled. The FETs are placed on the top layer and the second layer is a ground plane. The parasitic impedance Z2 between C_{IN} GND pad and M2 source pad is part of the hot loop and is studied as an example. Z2 is extracted from FastHenry. Table 3 summarizes and compares the simulated ESR2 and ESL2 with different via placements.

In general, adding more vias reduces the PCB parasitic impedance. However, the reduction of ESR2 and ESL2 is not linearly proportional to the number of vias. The vias close to the terminal pads give the most obvious reduction in PCB ESR and ESL. Therefore, for hot loop layout design, several critical vias must be placed close to the pads of C_{IN} and MOSFETs to minimize the HF loop impedance.

Case	ESR_2 (mΩ) at 2 MHz	ESR Change Rate vs. Initial Case	ESL_2 (nH)at 200 MHz	ESL Change Rate vs. Initial Case
Initial Case Without Vias	2.67	N/A	1.19	N/A
(a)	1.73	–35.2%	0.84	–29.8%
(b)	1.68	–37.1%	0.82	–30.8%
(c)	1.67	–37.5%	0.82	–31%
(d)	1.65	–38.2%	0.82	–31.4%

Table 3: Extracted Hot Loop PCB ESR2 and ESL2 with Different Via Placements

Conclusion

The reduction of a hot loop's parasitic parameters can help improve the power efficiency, lower voltage ringing, and reduce the EMI. To minimize the PCB parasitic parameters, hot loop layout designs with different decoupling capacitor positions, MOSFET sizes and positions, and via placements were studied and compared. A shorter hot loop path, smaller sized MOSFETs, symmetrical 90˚ shape and 180˚ shape MOSFETs placements, and vias close to the key components contribute to the lowest hot loop PCB ESR and ESL.

References

1 Mattan Kamon, Michael Tsuk, and Jacob White. "FASTHENRY: A Multipole-Accelerated 3-D Inductance Extraction Program." IEEE Transactions on Microwave Theory and Techniques, Vol. 42, 1994.

2 Andreas Musing, Jonas Ekman, and Johann W. Kolar. "Efficient Calculation of Non-Orthogonal Partial Elements for the PEEC Method." IEEE Transactions on Magnetics, Vol. 45, 2009.

3 Ren Ren, Zhou Dong, and Fei Fred Wang. "Bridging Gaps in Paper Design Considering Impacts of Switching Speed and Power-Loop Layout." IEEE, 2020.

4 Yonghwan Cho and Keith Szolusha. "4-Switch Buck-Boost Controller Layout for Low Emissions—Single Hot Loop vs. Dual Hot Loop." Analog Dialogue, Vol. 55, July 2021.

5 Henry J. Zhang. "PCB Layout Consideration for Non-Isolated Switching Power Supplies." Analog Devices, Inc., 2012.

6 Christian Kueck. "Power Supply Layout and EMI." Analog Devices, Inc., 2012.

It is Easy to Drive & Protect SiC MOSFET

More than ten years ago, we started seeing increasing Silicon Carbide (SiC) Metal–Oxide–Semiconductor Field-Effect Transistors (MOSFETs) activities and a splash of product launches from key power semiconductor suppliers like Cree and Infineon. At the same time, many new suppliers were trying to dethrone the incumbent silicon and change the gameplay in their own ways. However, this is a mammoth task as Insulated-Gate Bipolar Transistors (IGBTs), which have been around for more than 40 years, are too entrenched in every power electronics engineer's design.

By Chun Keong Tee, Product Manager of Isolation Products Division, Broadcom Inc.

Introduction

Although SiC MOSFETs can bring forth many benefits, it took more than ten years for the suppliers to consolidate and align SiC MOSFET specifications and standards. These include the definitions of driving and protecting the SiC MOSFET. For example, there was the normally "ON" SiC Junction-Gate Field Effect Transistor (JFET) that will need a negative gate voltage to turn it off. There was also the more acceptable normally "OFF" switch but will require very high gate voltage of 20 V to ensure low conduction loss. Then, engineers had to redesign their power supply, which has been optimized for the IGBT at 15 V gate-emitter voltage (V_{GE}). This is just one of the problems, not to mention other challenges like high-speed operation and dv/dt noise when SiC MOSFETs switch faster.

Today, most of the disparities have been aligned to very much how we will drive IGBTs. Most importantly, gate drive technologies have also improved tremendously to catch up and enable the adoption of SiC MOSFETs. Broadcom newly released a 10 A gate drive optocoupler, the ACPL-355JC. It is able to fulfil the demanding requirements of driving and protecting SiC MOSFETs.

At the same time, most of the major suppliers in power semiconductor industry are ramping up their SiC MOSFET production with packages and pinouts that can replace existing IGBTs easily. This drives the costs of SiC MOSFETs to a very competitive level, which is probably the most important factor that makes SiC MOSFET adoption take off.

The Standardization of SiC MOSFET Specifications

Broadcom gate driver optocoupler has evolved to meet the demand of SiC MOSFETs. Similarly, SiC MOSFETs have also evolved to be easily driven and protected by gate drivers. This section highlights some of the important changes in specification, which enable the growing adoption of SiC MOSFETs.

Figure 1: Infineon EasyDUAL™ 1B SiC MOSFET Module Driver Board

The first specification would be gate-source voltage, V_{GS}. Over the years, the optimum V_{GS} for SiC MOSFET operations has reduced from 20 V to 18 V and finally settled to the same level as the V_{GE} of IGBTs, at 15 V. This made the definition of our gate driver power supply and under voltage lockout (UVLO) threshold more definite.

The ACPL-355JC gate drive optocoupler has a wide supply range from 0 to 30 V, which makes it very versatile for either unipolar gate driving or bipolar gate driving. These ensure the SiC MOSFETs are firmly switched on or off. The ACPL-355JC's UVLO is set to 13 V which is suitable to drive most of the latest SiC MOSFETs' gates, which are designed to operate at 15 V V_{GS}.

The second specification is the total gate charge, Q_G. Q_G of SiC MOSFETs is more than 2 times smaller to their equivalent IGBT counterparts. This allows SiC MOSFETs to switch very quickly, reducing the switching losses and increasing the operating frequency. A lower Q_G also implies a lower gate current requirement, which helps to eliminate an additional current buffer stage. The ACPL-355JC has a 10 A peak driving current that can help overcome the input capacitance and charge up the SiC MOSFET's gate quickly. This optimizes the potential of the SiC MOSFET and improves the overall system efficiency.

The third specification is the slew rate or dv/dt which measures how fast the SiC MOSFET switches from zero to the BUS voltage within the shortest time. Although fast switching is critical to reduce switching losses, the high dv/dt generated can be a nuisance and cause noise to the SiC MOSFET control. The ability for the gate driver to reject the dv/dt noise is specified by the common mode transient immunity (CMTI). SiC MOSFETs are capable to switch 100 V/ns and the ACPL-355JC has a CMTI rating to guarantee a noise immunity of more than 100 kV/µs.

The last specification is the short circuit withstand time (SCWT) of the SiC MOSFET. Silicon IGBTs in general have superior SCWTs to SiC MOSFETs. Hence, any short circuit fault current in the SiC MOSFET needs to be extinguished faster before the switch is destroyed. Typically, the rule of thumb is 1 to 3 µs for SiC MOSFETs, as compared to 5 to 10 µs for IGBTs. In terms of short circuit protection, the ACPL-355JC uses the same methodology as DESAT sensing of the IGBTs. The ACPL-355JC monitors the drain and source of the SiC MOSFET and triggers a soft shutdown when a high fault current increases the drain source voltage. To address the difference in time, how fast the SiC MOSFET and IGBT need to be protected, the detection voltage, detection time and shutdown time of the ACPL-355JC can be adjusted using external discreet components.

Driving and Protecting SiC MOSFET Modules in Standard Packages

This section will look into driving 1200 V SiC MOSFETs from two major suppliers, in standard module packages for low and high current:

Supplier	Part Number	Package	Current Class
Infineon	FF11MR12W1M1	EasyDUAL™ 1B	100 A
Wolfspeed	WAB300M12BM3	62 mm	300 A

Table 1: 1200 V SiC MOSFET Modules in Standard Packages for Different Current Classes

Infineon FF11MR12W1M1 1200 V/100 A SiC MOSFET Module

Figure 1, shows the driver board which features two gate drive optocouplers ACPL-355JC, for driving a SiC MOSFET module in EasyDUAL™ 1B package. The board has an integrated capacitor DC bus, isolated switch mode power supplies (SMPS) for the gate drivers and access to pulse width modulated (PWM) inputs and short circuit fault signals.

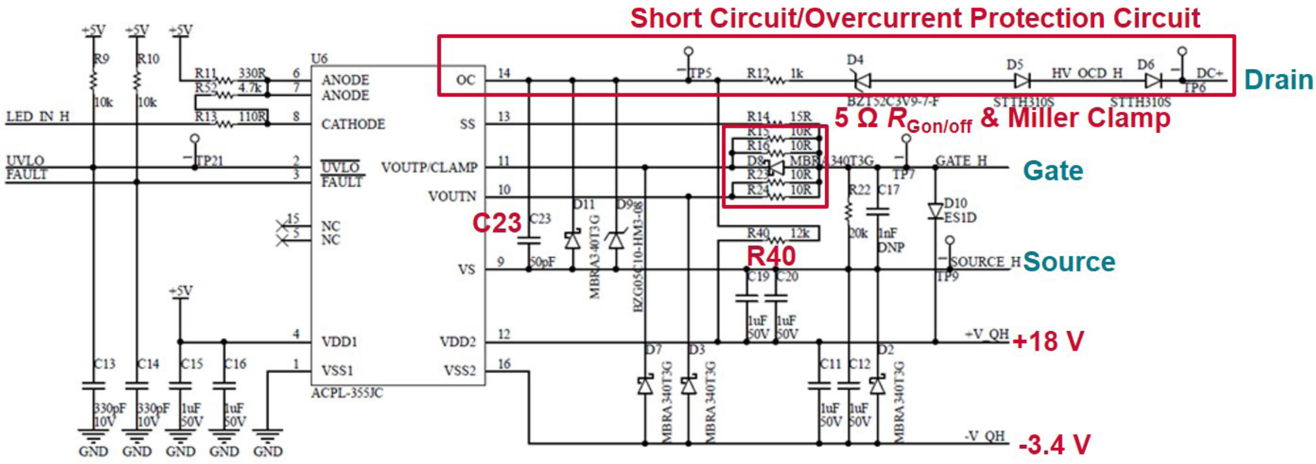

Figure 2: Infineon EasyDUAL™ 1B SiC MOSFET Module ACPL-355JC Gate Driving Circuitry

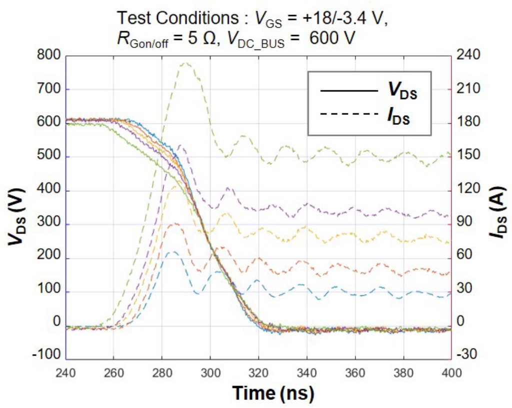

Figure 3: Infineon's FF11MR12W1M1 SiC MOSFET Module Turn-on Switching Waveforms

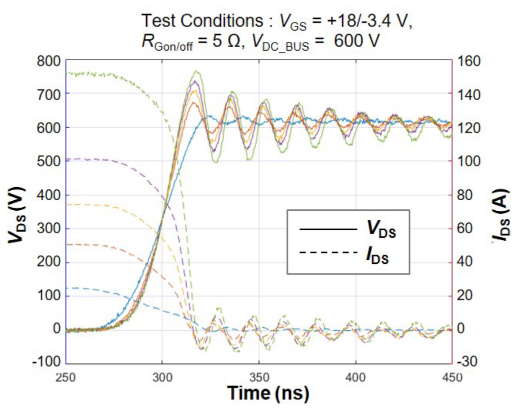

Figure 4: Infineon's FF11MR12W1M1 SiC MOSFET Module Turn-off Switching Waveforms

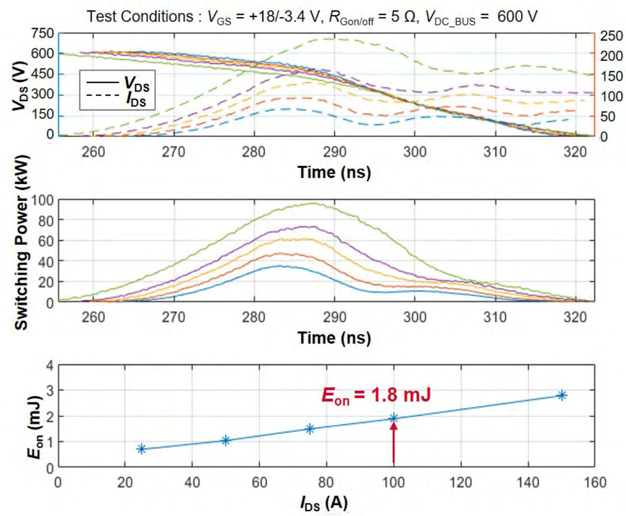

Figure 5: Infineon's FF11MR12W1M1 SiC MOSFET Module Turn-on Switching Energy Losses

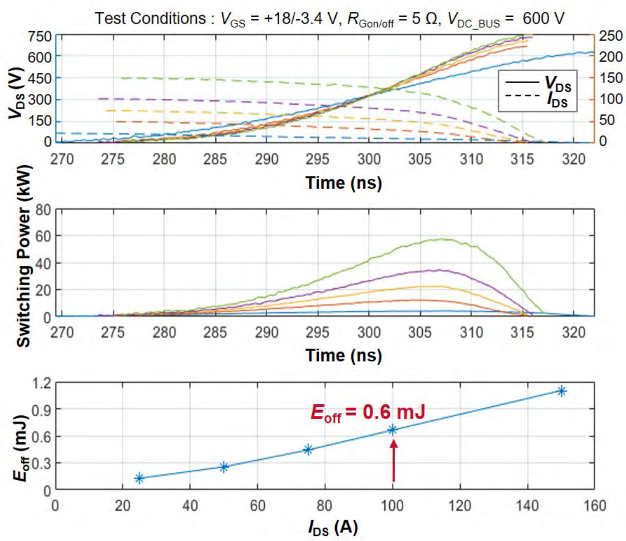

Figure 6: Infineon's FF11MR12W1M1 SiC MOSFET Module Turn-off Switching Energy Losses

The isolated SMPS, which serves as the ACPL-355JC secondary side power supply, is designed for bipolar driving of the gate at +18 V and -3.4 V. This is recommended by the Infineon application note AN2018-09, for high frequency switching.

The ACPL-355JC has two outputs, VOUTP and VOUTN which are connected to 5 Ω gate resistances for positive and negative gating. The 5 Ω gate resistances are realized with two parallel resistors to increase the power dissipation capability. The resulting peak current is approximately 4 A, which is lower than ACPL-355JC's peak limit of 10 A. In addition, the Schottky diode D8, placed between gate and VOUTP pin, is used together with CLAMP function to shunt parasitic Miller current during the off cycle.

Using this driving circuit, the switching waveforms of Infineon's FF11MR12W1M1 are measured using the double pulse test at 600 V V_{DC_BUS}. Figure 3 and Figure 4, show the turn-on and turn-off switching transients at different drain current levels I_{DS}.

The instantaneous power during switching and the resulting switching energy losses can be calculated as shown in Figure 5 and Figure 6. Based on the switching energies of 1.8 mJ (E_{on}) and 0.6 mJ (E_{off}) at 100 A, the switching performance measured is on par with what is specified in Infineon's datasheet.

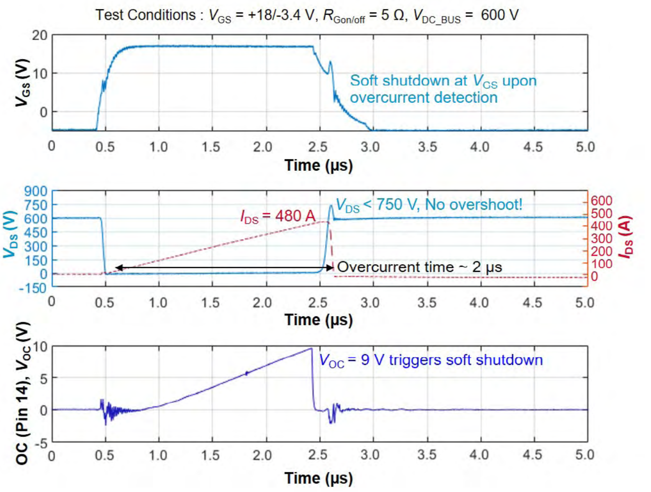

Figure 7: Infineon's FF11MR12W1M1 SiC MOSFET Module Overcurrent Protection

In Figure 2, the ACPL-355JC and its short circuit and overcurrent protection circuit, made up out of OC (Pin 14), Zener diode (D4) and high voltage blocking diodes (D5 and D6), is connected to the drain of the SiC MOSFET module. Using this connection, the ACPL-355JC senses if there is an increase in the V_{DS} over the SiC MOSFET in the event of a short circuit or over current condition. And depending on the blanking time which can be adjusted by C23 and R40, the speed of the high current fault detection can be adjusted. For example, the Infineon datasheet states that the short circuit duration should be kept under 2 µs to prevent the SiC MOSFET module from exceeding its package thermal dissipation.

Figure 7 shows the overcurrent protection waveforms done with a loop inductance of 2.5 µH. The current surged almost 5 times above the rated current of 100 A before being brought down to 0 A quickly within 2 µs. The shutdown at V_{GS} 18 V is completed softly via the ACPL-355JC softshut (SS) pin 13, to minimize the SiC MOSFET VDS overshoot that governs by, $V_{DS} = V_{DC\_BUS} - L_{par} * di/dt$ [7]. The soft shutdown lowers the negative di/dt, which causes the overshoot.

Figure 8: Wolfspeed 62 mm Half-Bridge SiC MOSFET Module Driver Board

Wolfspeed WAB300M12BM3 1200 V/300 A SiC MOSFET Module

This driver board also features two ACPL-355JC, for driving SiC MOSFETs in 62 mm housing. The board has an isolated SMPS for gate drivers and access to PWM inputs and short circuit fault signals.

WAB300M12BM3 has a higher current rating than FF11MR12W1M1. As such, a larger peak gate current is required to overdrive Q_G of the SiC MOSFETs. The isolated SMPS is designed for bipolar driving of the gate at +15 V and -4 V as recommended in the WAB300M12BM3 datasheet. To achieve a larger gate current, 2.95 Ω gate resistances are used for positive and negative gating. The 2.95 Ω gate resistances are realized with two parallel 5.9 Ω resistors to increase the power dissipation capacity. The resulting peak current is approximately 6 A, which is lower than ACPL-355JC's peak limit of 10 A.

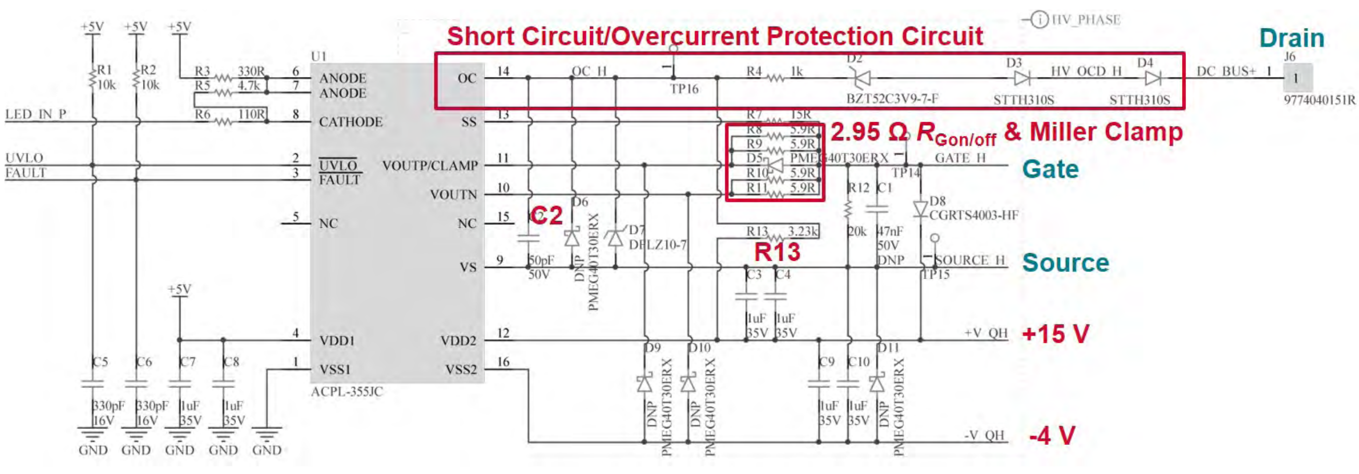

Figure 9: Wolfspeed 62 mm SiC MOSFET Module ACPL-355JC Gate Driving Circuitry


DANISENSE
YOU ASKED FOR IT...WE
MADE IT!
• 1000A rms
• 41,2mm Aperture
• Linearity better than 1ppm
www.danisense.com
DN1000ID

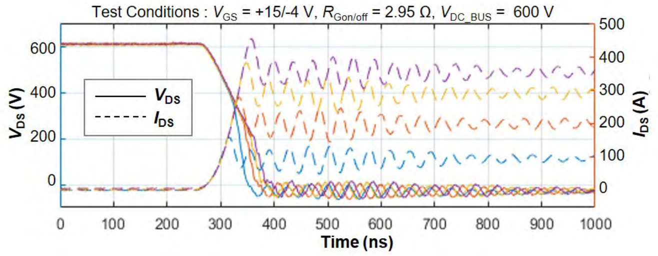

Figure 10: Wolfspeed's WAB300M12BM3 SiC MOSFET Module Turn-on Switching Waveforms

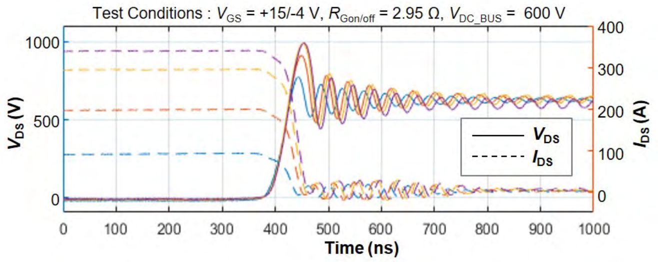

Figure 11: Wolfspeed's WAB300M12BM3 SiC MOSFET Module Turn-off Switching Waveforms

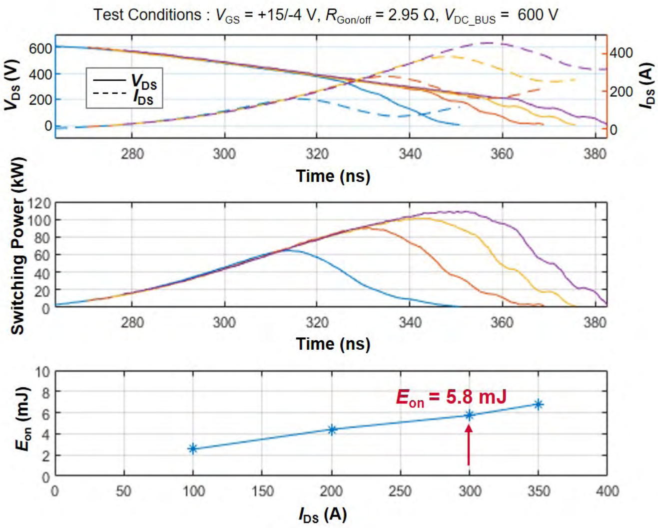

Figure 12: Wolfspeed's WAB300M12BM3 SiC MOSFET Module Turn-on Switching Energy Losses

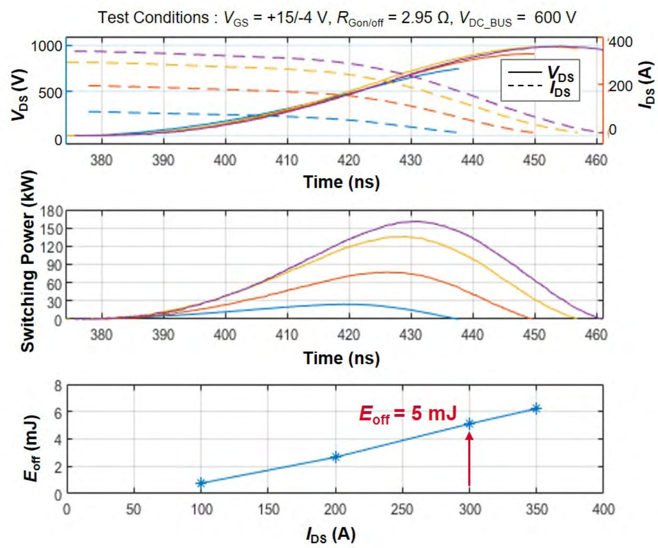

Figure 13: Wolfspeed's WAB300M12BM3 SiC MOSFET Module Turn-off Switching Energy Losses

Using this driving circuit, the switching waveforms of Wolfspeed's WAB300M12BM3 are measured using the double pulse test at 600 V V_{DC_BUS}. Figure 10 and Figure 11, show the turn-on and turn-off switching transient at different drain current levels I_{DS}.

The instantaneous power during switching and the resulting switching energy losses can be calculated as shown in Figure 12 and Figure 13. Based on the switching energies of 5.8 mJ (E_{on}) and 5 mJ (E_{off}) at 300 A, the switching performance measured is on par with what is specified in Wolfspeed's datasheet.

In Figure 9, the ACPL-355JC and its short circuit and overcurrent protection circuit, made out of OC (Pin 14), Zener diode (D2) and high voltage blocking diodes (D3 and D4), is connected to the drain of the SiC MOSFET. Using this connection, the ACPL-355JC senses if there is an increase in V_{DS} over the SiC MOSFET in the event of a short circuit or overcurrent condition. And depending on the blanking time which can be adjusted by C2 and R13, the speed of the high current fault detection can be adjusted.

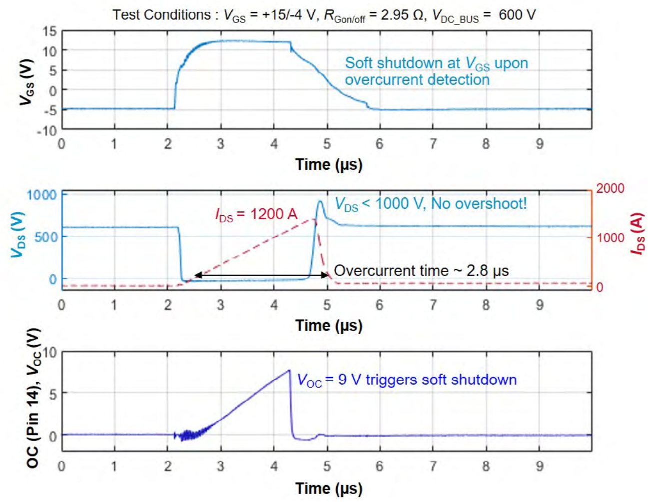

Figure 14: Wolfspeed's WAB300M12BM3 SiC MOSFET Module Overcurrent Protection

Figure 14 shows the overcurrent protection waveforms done with a loop inductance of 1.5 µH. The current surged to 4 times above the rated current of 300 A before being brought down to 0 A quickly within 3 µs. The shutdown at V_{GS} 15 V is completed softly via the ACPL-355JC softshut (SS) pin 13, to minimize the SiC MOSFET VDS overshoot

Conclusion

This article demonstrates the driving and protection of 1200 V SiC MOSFETs from two different suppliers with different current ratings and module packages. With the unification of SiC MOSFETs specifications and the ACPL-355JC's versatility in terms of output gate voltage, driving current and adjustable short circuit or overcurrent detection time, it is easy to drive and protect SiC MOSFETs now.

References

1. Datasheet " FF11MR12W1M1_B11 EasyDUAL™ Modul mit CoolSiC™ Trench MOSFET und PressFIT / NTC," Infineon Technologies AG, V2.2 2018-07-18.
2. "Guidelines for CoolSiC™ MOSFET gate drive voltage window," Infineon Technologies AG, AN2018-09 version 1.2
3. Datasheet " WAB300M12BM3 1200 V, 300 A All-Silicon Carbide THB-80 Qualified, Switching Optimized, Half-Bridge Module," Cree Inc, Rev A, 2020-05-20.
4. Datasheet "ACPL-355JC 10A IGBT and SiC MOSFET Gate Drive Optocoupler with Integrated Overcurrent Sensing, FAULT, and UVLO Status Feedback," Broadcom Inc, ACPL-355JC-DS101.
5. Reference Manual " ACPL- 355JC DUAL 1B SiC Module EB1200-355JC Evaluation Board," Broadcom Inc, ACPL-355JC-Dual1B-RM101 Version 1.1.
6. Reference Manual " ACPL-355JC 62-mm SiC Module EB1200M62-355JC Evaluation Board," Broadcom Inc, ACPL-355JC-62mmSiC-RM100 Version 1.0.
7. Thomas Basler, " Ruggedness of High-Voltage IGBTs and Protection Solutions," Universitätsverlag Chemnitz, 2014.

www.broadcom.com

A Comparative Study of the Thermal Performance of Different Die-Attach Materials Including a Preform-Based Diffusion Solder

Along with silver sintering, transient liquid phase soldering (TLPS) is considered as a replacement technology for bonding using high reliability solder alloys. Our Preforms for Diffusion Soldering PFDS400® were designed as a solution to the industrial application of TLPS technology. In this paper the thermal impedance of different variants of PFDS400® are compared with those of other die attach materials including those obtained using silver sintering to gain an insight into its thermal performance.

By Dmytro Pavlyuchkov & Ralph Mädler, Pfarr Stanztechnik GmbH

Introduction

Transient Liquid Phase Soldering (TLPS) technology is considered as an alternative to soldering using high reliability solder alloys (e.g. Sb-containing solders, AuSn20 etc.). The end-of-life and mechanical characteristics of such bonds based on Sn-Cu system exhibits behaviours comparable to those obtained using the silver sintering die-attach technology [1,2]. At first glance, the obvious drawback of TLPS joint might be the low thermal conductivity compared to that of sintered silver caused by the low thermal conductivity of Sn-Cu intermetallics. Literature data regarding the thermal properties of TLPS materials are scarce, especially in a layered form. Given the recent promising results of reliability studies on the die bonds obtained using our preform based diffusion solder material PFDS400® [3], the results of thermal resistance analysis may complement the overall picture of its capabilities as a die-attach material. In order to gain an idea about the thermal performance of the latter a thermal impedance comparative study of different bond materials was performed. This inspection method, well-known in Power Electronics, provides inferences on the thermal resistance of layers beneath the power semiconductor element of a power module stack. In this study we obtained and compared Z_{th}-characteristics for joints bonded using different types of PFDS400® with those bonded using conventional solders and silver sintering.

Material description and sample built up

For the Z_{th}-measurements six types of assemblies were manufactured using power diodes (SEMIKRON CAL-DIODE SKCD 61 C 170 I HD) in the dimension of 7.8 mm x 7.8 mm and two different substrates. The first type was bare copper DCB consisting of Cu/Al_2O_3/Cu layers with thicknesses 300 µm/ 380 µm/ 300 µm respectively. The second type was an Ag-thick-film substrate (Fraunhofer IKTS Systemintegration und AVT) with layers Ag/Al_2O_3 of 9 µm und 380µm thickness respectively. The diode backside metallization consisted of Ni/Ag layers. The front side metallization consisted of a bondable Al layer. The overall die thickness was 304 µm. The following die-attach materials were used: solder preforms of SnAg3.5 and SnAg3.0Cu0.5, a family of preform based diffusion solders PFDS400®M and silver paste (for silver sintering). Solder preforms of SnAg3.5 and SnAg3.0Cu0.5 alloys were modified using integrated spacer wires in order to guarantee a homogeneous bond line thickness comparable to the other joints. This type of preform belongs to the family WireGuard® preforms designed by Pfarr Stanztechnick GmbH. The reflow soldering and TLPS bonding of semiconductors was performed by PINK GmbH Thermosysteme using their VADU vacuum reflow soldering system. The silver sintering was performed by PINK GmbH Thermosysteme using a SIN sintering system. Scanning acoustic microscopy (C-SAM) was used to examine the joints for void formation. For the Z_{th}-measurement 7 samples of each material configuration were built up. After the Z_{th}-measurements microstructures of each connection type were studied using cross-sectional analysis. The die-attach material and the substrate type used are presented in Table 1.

Joint Quality and Material Characterization

The C-SAM images shown in Figure 1 demonstrate a high quality for all joints manufactured for this study, exhibiting a low degree of void formation.

The two contrasting strips visible in Figure 1a correspond to the location of the spacer wires of SnAg3.5 and SnAg3Cu0.5 solder preforms.

Figure 2 shows cross sectional images corresponding to the joints shown in Figure1. The microstructures confirm the high joint-quality demonstrating a dense structure with a low degree of micropo-

Die attachement material	Type	Thickness [µm]	Substrate Type
SnAg3.5 - WireGuard®	Preform with integrated spacer wires	50	Bare Cu-DCB
SnAg3.0Cu0.5 - WireGuard®	Preform with integrated spacer wires	50	Bare Cu-DCB
PFDS400®M/Cu	TLPS preform, Cu-Sn-System	50	Bare Cu-DCB
PFDS400®M/Ni-Cu	TLPS preform, Cu-Ni-Sn-System	50	Bare Cu-DCB
Silver Sinter Paste	Paste (Externally supplied material)	20-25	Bare Cu-DCB
PFDS400®M/Ag	TLPS preform, Ag-Sn System	30	Ag Thickfilm Substrate
Silver Sinter Paste	Paste (Externally supplied material)	20-25	Ag Thickfilm Substrate

Table 1: Compared test vehicles; consisting of the die attachment material, its layer thickness and the substrate type used.

rosity in both silver-sintered and TLPS joints as well as in conventional solder joints. The TLPS joints characterised by the formation of a number of Sn-containing intermetallic compounds providing their high-temperature mechanical stability. Depending on the assembled parts and their metallization the following intermetallics were formed: Cu6Sn5, Cu3Sn, Ag3Sn, Ni3Sn4. The formation of intermetallics was also observed in the SnAg3.5 and SnAg3Cu0.5 joints at the location of the Cu wire spacer (Figure 2a). Based on the cross-sectional analysis, the total joint thickness was determined and summarized in Table 1 together with supplementary information.

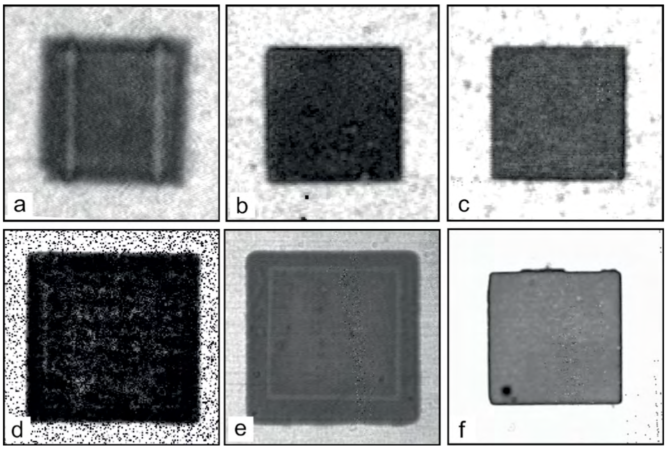

Figure 1: C-SAM images of the die-attach joints (material-substrate): a) SnAg3.5 or SnAg3Cu0.5 WireGuard® preforms - DCB; b) PFDS400®M/Cu - DCB; c) PFDS400®M/Ni-Cu - DCB; d) sintered Ag - DCB; e) sintered silver - Ag-thick-film substrate; f) PFDS400®M/Ag - Ag-thick-film substrate.

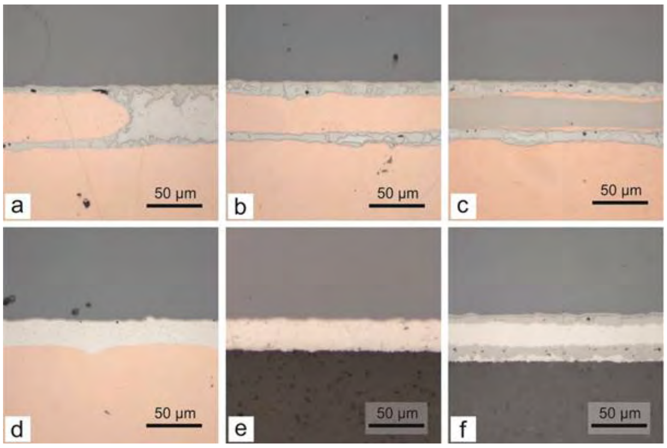

Figure 2: Cross-sectional images of the die-attach joints (material-substrate): a) SnAg3.5 or SnAg3Cu0.5 WireGuard® preforms - DCB; b) PFDS400®M/Cu - DCB; c) PFDS400®M/Ni-Cu - DCB; d) sintered silver - DCB; e) sintered silver - Ag-thick-film substrate; f) PFDS400®M/Ag - Ag-thick-film substrate.

Measurement procedure

The measurement of the thermal impedance Z_{th} of power electronic devices is based on the heat flow between the source of the dissipated power (e.g. a power chip) and a reference point. This reference point can be set at the underside of the device (case), at the heat sink or at the ambient temperature, respectively. During the measurement procedure the device is heated up by the implementation of a constant load current for a specific on-time. At the end of the heating phase the power loss is determined by measuring the voltage drop and load current. When the current is switched off the measurement of T_j and T_{ref} is started and tracked until a constant temperature is reached. The temperature-dependent voltage drop of the pn junction of the chip is used as a temperature sensitive electrical parameter (TSEP) by introducing a sufficiently small measurement current into the device to prevent self-heating.

For the calculation of the thermal impedance equation (1) is used:

$$Z_{th}(t) = \frac{T_j(t) - T_{ref}(t)}{P_V} \tag{1}$$

To obtain the desired Z_{th} function, the cooling curve ($Z_{th,down}$) must be converted into a heating curve ($Z_{th,up}$). By use of equation (2) with R_{th} estimated at the time point with the highest measured temperature this conversion is completed.

$$Z_{th,up}(t) = R_{th} - Z_{th,down} \tag{2}$$

With the help of thermal simulations, the time constants of the different layers can be estimated. With this knowledge, an evaluation of the thermal impedance of the solder or sinter layer, respectively is performed at about 5-15 ms.

Results and Discussion

Using the measurement procedure described above, Zth functions were obtained for die-bonding with DCB-substrates (Figure 3) and with Ag thick film (Figure 4)

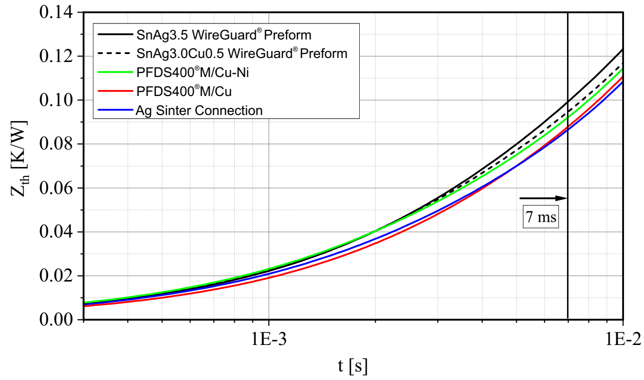

a)

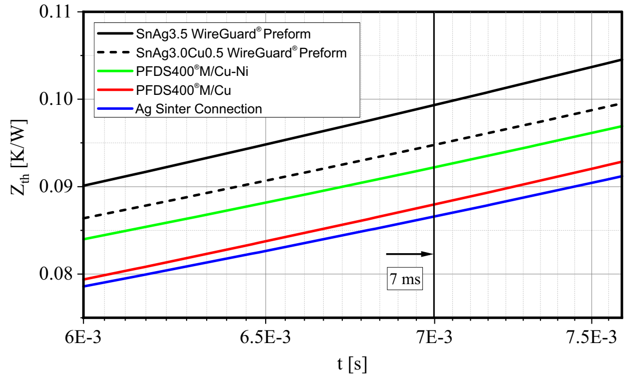

b)

Figure 3 a) Z_{th} curves of the die-attach joints with DCB b) Z_{th} functions of the die-attach joints with DCB on a timescale in the vicinity of 7ms

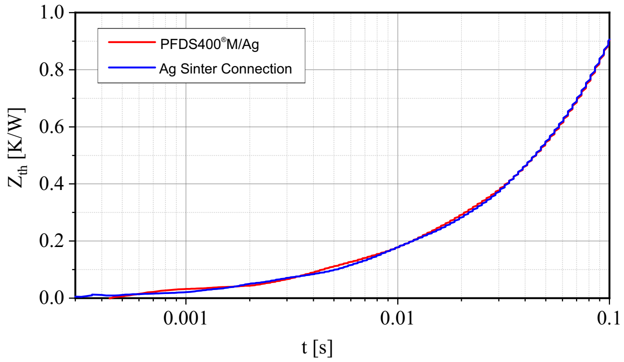

Figure 4: Zth-curves of the die-attach joints with Ag-thick-film

For a close comparison of the Zth functions of the die-attach joints with DCB shown in Fig.3b, a smaller area around the 7ms time constant was considered, where the influence of the bonding material was assumed. The Zth values detected at 7ms are summarized in Table 2.

Material	Z_{th}-value around 7 ms [K/W]
SnAg3.5 WireGuard®	0,0993
SnAg3Cu0.5 WireGuard®	0,0948
PFDS400®M/Cu-Ni	0,0921
PFDS400®M/Cu	0,0879
Silver Sintering	0,0865

Table 2: Z_{th} values for the die bonding with DCB-substrates measured at 7ms

Comparison of the Z_{th} functions reveals very little difference (0.0014 K/W at 7 ms) between those of the 25 µm thick silver sintered joints and those of the 50 µm thick PFDS400®M/Cu diffusion soldered joints on the Cu-DCB carrier. At the same time no noticeable difference in Zth values was observed between 30 µm thick PFDS400®M/Ag and a 25 µm thick silver sintered connection on the Ag-thick-film substrate. The SnAg3.5 and SnAg3Cu0.5 WireGuard® preforms show higher Zth values demonstrating elevated thermal resistivity compared to other bond materials, which is expected for tin-based solders. The PFDS400®M/Ni-Cu material exhibits reduced thermal performance compared to the copper-containing PFDS400® variant, as it contains more of the less thermally conductive Ni compared to highly conductive Cu. Nevertheless, PFDS400®M/Ni-Cu exhibits lower thermal impedance compared to SnAg3.5 and SnAg3Cu0.5 WireGuard® preforms. Despite the multi-layered structure of PFDS400® preforms and thus the presence of numerous thermoresistant boundaries, this material demonstrates a thermal performance comparable to Ag-sintered joints. This is regardless of the fact, that the Ag-sintered joints shown in Figure 1 d,e and Figure 2 d,e exhibit fairly good sintered structures with a minimal degree of porosity. Although the joints with PFDS400®M/Cu and PFDS400®M/Ag are almost twice as thick as Ag-sintered joint, they exhibit comparable thermal resistance.

Conclusions

In this article a comparative analysis of thermal impedance measurements of different die-attach materials was performed. The results have shown that despite the layered structure and thicker joint gap, the PFDS400® material, namely the PFDS400®M/Cu and PFDS400®M/Ag variants exhibited values comparable to silver sintered joints. PFDS400®M/Cu-Ni exhibited higher thermal resistivity due to the reduced thermal conductivity of the Ni layer, albeit lower compared to SnAg3.5 and SnAg3Cu0.5 solders. Given that the reliability of semiconductor solder joints with PFDS400® is as good as that of sintered silver, the results of this work indicate that this material offers a better alternative to high-reliability, lead-free solders and competes head-to-head with silver sintering technology.

References

[1] A. Otto et al., "Evaluation of Ag-sinter and CuSn-TLP based joining technologies on lead frame", PCIM Europe 2018, Nuremberg, Germany
[2] K. Guth et al., "End-of-life investigation on the .XT interconnect technology" PCIM Europe 2015, Nuremberg, Germany
[3] B. Ottinger et al., "Reliability of lead-free solders for die attach in automotive power modules", 2022 IEEE 24th Electronics Packaging Technology Conference, Singapore, Singapore.

Acknowledgement

We would like to thank the Power Electronics Group of Chemnitz University of Technology for conducting the Zth measurements and for their support in the interpretation of the results. We would also like to thank the Systems Integration and Electronic Packaging Group of Fraunhofer IKTS and the company Pink GmbH Thermosysteme for providing materials, carrying out the joining processes and the inspection of the samples.

www.pfarr.de

Power Quality Monitoring Part 1: The Importance of Standards Compliant Power Quality Measurements

This article discusses the importance of power quality (PQ) measurements in today's electric infrastructure and reviews areas of application for PQ monitoring. It will cover the IEC standard for power quality and its parameters. Finally, it summarizes the key differences between Class A and Class S power quality meters. A subsequent article will illustrate recommended solutions on "How to Design a Standards Compliant Power Quality Meter."

By Jose Mendia, Senior Engineer, Product Applications, Analog Devices

The Need for Power Quality Measurement in Today's Electric Infrastructure

Power quality has found a renewed interest due to changing power generation modes and consumption dynamics. The unprecedented growth in renewable sources at different voltage levels has increased the amount of PQ related issues. Consumption patterns have also seen a wide transformation due to unsynchronized loads added at multiple entry points of the grid and voltage levels. Some examples are electric vehicle (EV) chargers that can require hundreds of kilowatts and a great number of data centers and their related equipment such as heating, ventilation, and air conditioning. In industrial applications, arc furnaces that run by variable frequency drives, switching transformers, etc. not only add a lot of unwanted harmonics to the grid, but are also responsible for voltage dips, swells, transient brownouts, and flicker.

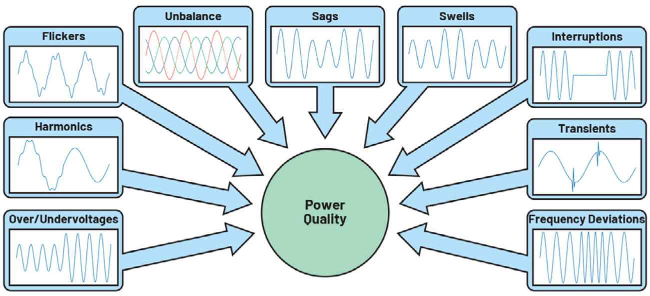

Figure 1: Power quality issues.

Power quality in the utility space refers to the quality of the voltage delivered to the consumer; a series of prescribed regulations for the magnitude, phase, and frequency determine this quality of service. However, by definition, it denotes both voltage and current. While the voltage is easily controlled by the generation side, the current is governed largely by consumer usage. The concept and implications of PQ issues are rather widespread depending on the end users.

The economic impact of bad PQ has been studied and surveyed extensively in the last few years; its effects are estimated to be in the region of billions of dollars worldwide.[1] All these studies conclude that monitoring the quality of power has a direct impact on the economic results of many business sectors. Even though it is clear how bad PQ negatively affects the economics of business, monitoring it efficiently and effectively at scale is not an easy task. Monitoring PQ in a facility involves having highly trained personnel and expensive equipment installed on multiple points along the electric system for long or indefinite periods of time.

Power Quality Monitoring Areas of Application

Power quality monitoring is often seen as a cost saving strategy for some business sectors and a critical activity for others. Power quality issues can arise in a broad range of electric infrastructure, as illustrated in Figure 2. As we'll discuss later, power quality monitoring is becoming increasingly critical in business sectors such as electric generation and distribution, EV charging, factories, and data centers.

Electricity Utility Companies, Electricity Transmission, and Distribution

Utility companies serve the consumers with distribution systems that include generating stations, which are power substations that supply electricity via transmission lines. The voltage supplied via these transmission lines is stepped down to lower levels by substation transformers, which inject certain harmonics or interharmonics to the system. Harmonic currents in distribution systems can cause harmonic distortion, low power factor, and additional losses as well as overheating in the electrical equipment[2], leading to a reduction in the lifetime of equipment and increases in cooling costs. Nonlinear single-phase loads served by these substation transformers deform the current's waveform. The unbalance of nonlinear loads leads to additional losses on power transformers, additional load of neutrals, unexpected operation of low power circuit breakers, and incorrect measurement of electricity consumed.[3] Figure 3 illustrates the effect of these linear loads.

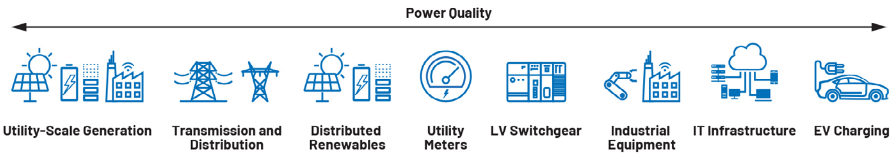

Figure 2: The dynamics of generation and consumption can lead to power quality issues across electric infrastructure.

Electricity generation by wind and photovoltaic (PV) solar systems injected into the grid cause several power quality problems as well. On the wind generation side, wind intermittency creates harmonics and short-duration voltage variations.[4] The inverters in PV solar systems create noise that can produce voltage transients, distorted harmonics, and radio frequency noise because of the high speed switching commonly used to increase the efficiency of the energy harvested.

EV Chargers

EV chargers can face multiple power quality challenges, both in power sent to and from the grid (see Figure 4). From a power distribution company perspective, power electronics-based converters used in EV chargers inject harmonics and interharmonics. Chargers with improperly designed power converters can inject direct currents (DC). Additionally, fast EV chargers introduce rapid voltage changes and voltage flicker into the grid. From the EV charger side, faults in transmission or distribution systems lead to voltage dips or interruption of supply voltage to the charger. Reduction of voltage from the EV charger tolerance limits will lead to activation of undervoltage protection and disconnection from the grid (which leads to a very bad user experience).[5]

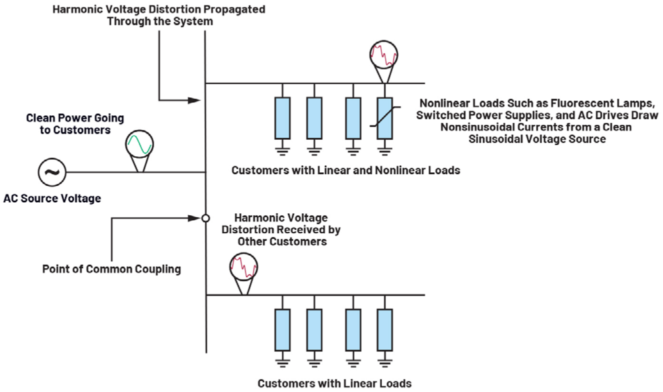

Figure 3: The impact of current harmonics generated by a nonlinear load.

Factories

Power quality problems caused by power supply variations and voltage disturbances, cost approximately $119 billion (U.S.) per year for industrial facilities in the United States, as per an Electric Power Research Institute (EPRI) report.[6] Additionally, 25 EU states suffer an equivalent of $160 billion (U.S.) in financial losses per year due to different PQ issues, according to the European Copper Institute.[7] These figures are linked to subsequent downtime and production losses as well as the equivalent of intellectual productivity losses.[8]

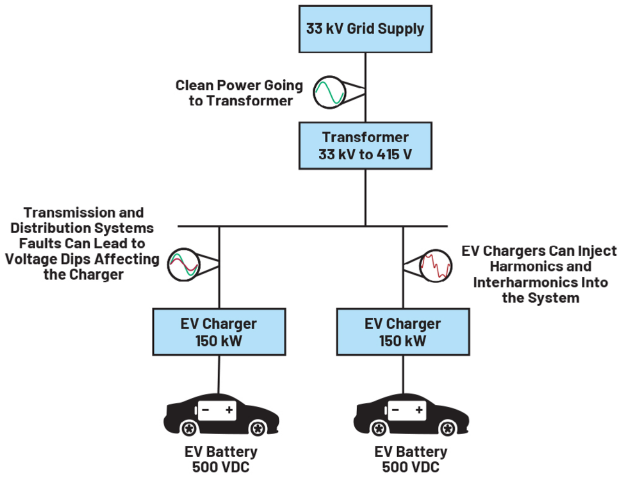

Figure 4: Power quality issues for EV chargers.

Degradation of power quality is usually caused by intermittent loads and load variations from arc furnaces and industrial motors. Such disturbances give rise to surges, dips, harmonic distortions, interruptions, flicker, and signaling voltages.[9] To detect and record these disturbances inside a factory installation, it is necessary to have power quality monitoring equipment in several points throughout the electric installation or, even better, have it at the load level. With the arrival of new Industry 4.0 technologies, power quality monitoring at the load can be addressed by industrial panel meters or submeters to have a comprehensive view of the quality of the power delivered to each load.

Data Centers

Presently, most business activities depend on data centers in one way or another to provide email, data storage, cloud services, etc. Data centers demand a high level of clean, reliable, and uninterrupted electricity supply. PQ monitoring excellence helps managers prevent costly outages and helps manage equipment maintenance, or replacement, required due to issues on the power supply units (PSU). The integration of uninterruptable power supply (UPS) systems into rack power distribution units (PDUs) represents another reason to add PQ monitoring to IT racks inside the data center. This integration can provide visibility to power issues at a power socket level.

UPS system failure, including UPS and batteries, is the primary cause of unplanned data center outages according to a report made by Emerson Network Power.[10] Around a third of all reported outages cost companies nearly $250,000.[11] UPS systems are used on every data center to ensure clean and uninterrupted power. These systems isolate and mitigate most of the power problems from the utility side, but they do not protect against issues generated by the PSU of IT equipment itself. IT equipment PSUs are nonlinear loads that can introduce harmonic distortion in addition to other problems caused by equipment such as those that can result in high density cooling systems with variable frequency speed-controlled fans. Apart from these issues, PSUs also face interferences that come in multiple forms such as voltage transients and surges, voltage swells, sags, and spikes, imbalance or fluctuations, frequency variation, and poor facility grounding.

Power Quality Standards Defined

Power quality standards specify measurable limits to the electricity magnitudes as to how far they can deviate from a nominal specified value. Different standards apply to different components of the electricity system. Specifically, the International Electrotechnical Commission (IEC) defines the methods for measurement and the interpretation of results of PQ parameters of alternating current (AC) power systems in the IEC 61000-4-30 standard. The PQ parameters are declared for fundamental frequencies of 50 Hz and 60 Hz. This standard also establishes two classes for measurement devices: Class A and Class S.

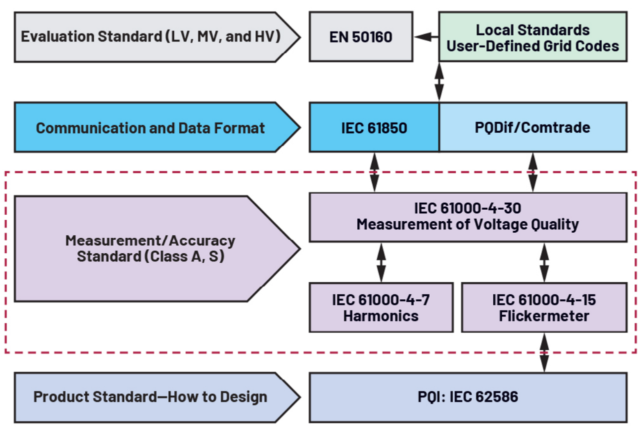

Figure 5: IEC power quality standards.

- Class A defines the highest level of accuracy and precision for the measurements of PQ parameters and is used for instruments requiring very precise measurements for contractual matters and dispute resolution. It is also applicable to the devices that need to verify compliance of the standard.
- Class S is used for power quality assessment, statistical analysis applications, and diagnostics of power quality problems with low uncertainty. The instrument in this class can report a limited subset of the parameters defined by the standard. The measurements made with Class S instruments can be done on several sites on a network, on complete locations or even on single pieces of equipment.

It is important to note that the standard defines the measurement methods, establishes a guide for the interpretation of the results, and specifies the performance of the power quality meter. It does not give guidelines on the design for the instrument itself.

The IEC 61000-4-30 standard defines the following PQ parameters for Class A and Class S measurement devices.[12]

Power frequency

- Magnitude of the supply voltage and current
- Flicker
- Supply voltage dips and swells
- Voltage interruptions
- Supply voltage unbalance
- Voltage and current harmonics and interharmonics
- Rapid voltage change
- Underdeviation and overdeviation
- Mains signaling voltage on the supply voltage

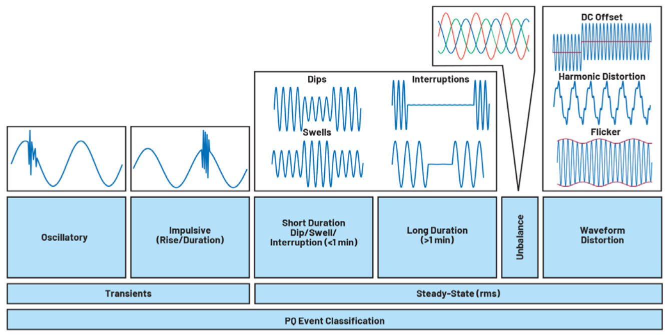

Figure 6: Classification of power quality parameters in a timescale.

	Class A	Class S
Voltage Measurement Accuracy	±0.1%	±0.5%
Current Measurement Accuracy	±1%	±2%
Voltage and Current rms Calculation	Half-cycle steps	One-cycle steps
Frequency Measurement Accuracy	±10 mHz	±50 mHz
150/180-Cycle Aggregation	No gaps permitted, synchronized with UTC 10 min tick	Gaps between aggregations allowed
Measurements of Harmonics up to Order	50th	40th
Time-Clock Uncertainty per 24 Hours	±1 second	±5 seconds
Time Synchronization	GPS receiver, radio timing signals or network timing signals	Not required
Operation Temperature Range	0°C to 45°C	Specified by manufacturer

Table 1: IEC 61000-4-30 Class A and Class S Key Differences.

Key Differences Between Class A and Class S Defined by the IEC 61000-4-30 Standard

Although Class A defines higher levels of accuracy and precision than Class S, the differences are beyond just levels of accuracy. Instruments must comply with requirements such as time synchronization, quality of probes, calibration period, temperature ranges, etc. Table 1 presents a list of requirements that instruments shall meet to be certified in one or the other class.

Conclusion

Power quality issues are present across the whole electric infrastructure. Having equipment that monitors these PQ issues helps to improve performance, quality of service, and equipment lifetime while reducing economic losses. In the subsequent article "How to Design a Standards Compliant Power Quality Meter," we will introduce an integrated solution and a ready to use platform that can significantly accelerate development and reduce costs for developing PQ monitoring products.

References

1 Panuwat Teansri, Worapong Pairindra, Narongkorn Uthathip Pornrapeepat Bhasaputra, and Woraratana Pattaraprakorn. "The Costs of Power Quality Disturbances for Industries Related Fabricated Metal, Machines and Equipment in Thailand." GMSARN International Journal, Vol. 6, 2012.

2 Sai Kiran Kumar Sivakoti, Y. Naveen Kumar, and D. Archana. "Power Quality Improvement In Distribution System Using D-Statcom in Transmission Lines." International Journal of Engineering Research and Applications (IJERA), Vol. 1, Issue 3.

3 Gabriel N. Popa, Angela Lagar, and Corina M. Diniş. "Some Power Quality Issues in Power Substation from Residential and Educational Buildings." 10th International Symposium on Advanced Topics in Electrical Engineering (ATEE), IEEE, 2017.

4 Sulaiman A. Almohaimeed and Mamdouh Abdel-Akher. "Power Quality Issues and Mitigation for Electric Grids with Wind Power Penetration." Applied Sciences, December 2020.

5 George G. Karady, Shahin H. Berisha, Tracy Blake, and Ray Hobbs. "Power Quality Problems at Electric Vehicle's Charging Station." SAE Transactions, 1994.

6 David Lineweber and Shawn McNulty. "The Cost of Power Disturbances to Industrial and Digital Economy Companies." Electric Power Research Institute, Inc., June 2001.

7 Roman Targosz and Jonathan Manson. "Pan-European Power Quality Survey." 9th International Conference on Electrical Power Quality and Utilisation, IEEE, 2007.

8 Subrat Sahoo. "Recent Trends and Advances in Power Quality." Power Quality in Modern Power Systems, 2020.

9A. El Mofty and K. Youssef. "Industrial Power Quality Problems." 16th International Conference and Exhibition on Electricity Distribution, 2001. Part 1: Contributions. CIRED (IEE Conf. Publ No. 482), IEEE, June 2001.

10 Cost of Data Center Outages." Ponemon Institute, January 2016.

11 Data Center Outages Are Common, Costly, and Preventable." Uptime Institute.

12 IEC 61000-4-30:2015: Electromagnetic Compatibility (EMC)-Part 4-30: Testing and Measurement Techniques-Power Quality Measurement Methods." International Electrotechnical Commission, February 2015.

About the Author

Jose Mendia has a B.Sc. in electronics and computer science engineering and joined the Energy and Industrial System Group at Analog Devices in 2016. Currently he is a senior engineer in product applications at the Edinburgh UK design center.

www.analog.com

High Reliability Alloy for Automotive Applications

Heraeus Electronics is pleased to announce the release of its Microbond® SMT660 Innolot® 2.0 no-clean printing T4 solder paste. The solder paste provides a competitive TCO offering. Based on Heraeus Electronics' proven experience, Innolot 2.0 allows a wide process window, enabling soldering in air with a low defect rate. Additionally, it is designed to offer an optimized formulation for lower costs.

With its approach through Microbond® SMT660 Innolot® 2.0 for highly reliable and cost-effective solder alloys for automotive applications, Heraeus Electronics introduces the ability to maintain a competitive Total-Cost-of-Ownership, while fulfilling emerging requirements. The next generation of Innolot® alloy offers reduced cost while maintaining the well-known features of higher creep resistance, resulting in longer product life cycles at higher operating temperatures. The Microbond® SMT660 Innolot® 2.0 solder paste performs in the air without additional N2 during reflow, while keeping defect rates low, reducing your TCO.

The flux Microbond® SMT660 uses an acrylic based synthetic resin eliminating potential batch-to-batch variations when using natural raw materials. Due to its low impurities and the flux design, a high

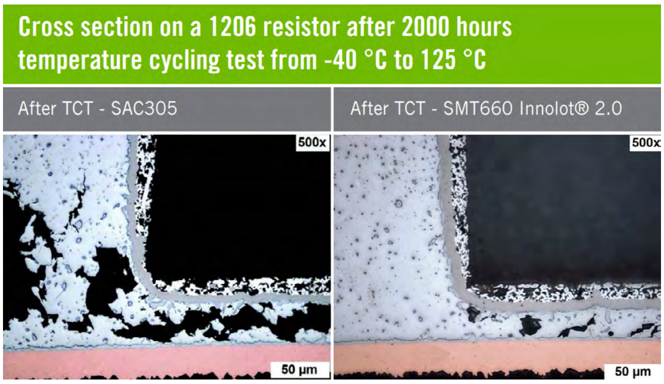

SIR performance is achieved. As a result, SMT 660 reduces the risk for electrochemical migration. The combination of the flux with Innolot® or Innolot® 2.0 alloy delivers a solder paste with superior reliability – especially in miniaturized systems in the automotive industry.

www.heraeus.com

Gallium Nitride Based 3-Phase Traction Inverter

VisIC Technologies Ltd. successfully tested its 2.2mΩ 650V half-bridge power module, consisting of 4 parallel 8mΩ Power FET, in a 3-phase configuration on a dyno-test-bench using a PMSM motor at a major automotive OEM. Thanks to this, VisIC Technologies has proven that their D³GaN (Direct Drive D-Mode Gallium-Nitride) semiconductor technology is well-suited even for the most challenging high-power automotive applications. Concerns about parallelization and oscillations caused by fast-switching transients have been addressed.

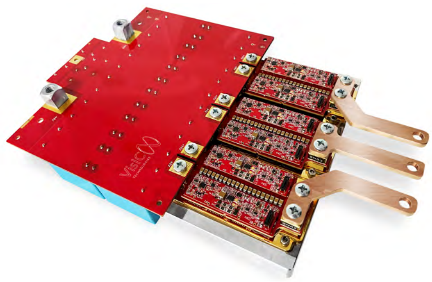

The inverter phase current reached 350Arms (500A peak) at 400V, although test system set-up limitations prevented higher currents, which the 2.2mΩ Power Module is capable of.

Worldwide Harmonized Light Vehicles Test Procedure (WLTP) driving cycle testing was executed and achieved comparable efficiency with commercial Silicon Carbide-based modules, despite using early non-optimized module prototypes. This means that D³GaN will deliver its promise of the highest efficiency, improving car costs through lighter, smaller power systems and a smaller battery size, without compromising the car's driving range. In addition, the D³GaN technology, based on GaN-on-Silicon semiconductor process, is delivering better than Silicon Carbide (SiC) performance at the more competitive Silicon cost level.

"With this great accomplishment, acknowledged by a leading automotive OEM, VisIC Technologies has provided overwhelming evidence for higher-efficiency at lower-cost future EV traction inverters, for the automotive world," said Dr. Tamara Baksht, CEO & Co-founder of VisIC technologies. "The automotive market demands high-power, high-voltage, high-reliability GaN, and our D³GaN die and module solutions are the answer."

VisIC Technologies 3-phase prototype inverter system will be available for testing across additional customer sites towards the end of the 2nd quarter of 2023.

www.visic-tech.com

ESD Protection Devices for a full spectrum of I/O Devices

Taiwan Semiconductor introduces the TESD Series of ultra-low-capacitance ESD protection devices. The Series comprises a wide selection of SMD components, providing single and multiple, unidirectional and bidirectional versions, for I/O ports (USB 2.0, USB 3.0, HDMI), audio systems, power ports and a variety of other ESD protection applications. The low capacitance topology of the TESD Series provides protection at high frequency data rates while maintaining signal integrity.

In I/O port applications, TESD Series devices meet regulatory requirements including repetitive application of IEC61000-4-2 (ESD) ±15kV (air), ±10kV (contact) and IEC61000-

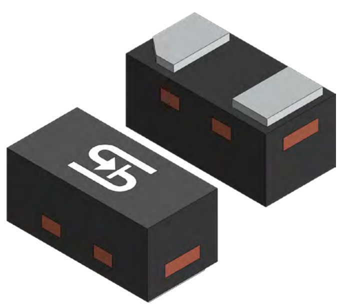

4-5 (Lightning): 5.5A (8/20µs). These devices also meet 30 KV contact/air requirements for power port applications. In addition, the Series meets all global environmental requirements. The devices' ultra-low capacitance is essential for ±3.3V or other nominal operating voltage applications operating at high data rates. The ESD protection devices ideally have little to no effect on normal operation while retaining the ability to survive repeated application of ESD discharges.

"By using these high-performance protection devices, the ESD is absorbed and safely clamped– dissipated through the TVS diodes – preventing expensive damage and increasing the reliability and survivability of the end equipment," said Sam Wang, Vice President, TSC Products. "This is achieved while also providing margin on protection and signal integrity."

www.taiwansemi.com

Expanded AC-DC Converter Offering

Bel Power Solutions announced its AC-DC converter series designed for industrial control equipment, machinery, and harsh environment applications. The series features cost-effective, energy efficient power supplies with standard DIN-rail mounting. LEC480 series has excellent EMC performance and is compliant with international IEC/EN/UL 62368, and UL 61010 safety standards. The products offer a high level of stability and immunity to noise for industrial control equipment, machinery, and other industrial applications in a variety of harsh environments. The AC-DC converters are available with output voltages of 12 V, 24 V, or 48 V (adjustable) with up to 480 watts of output power and an input voltage range of 85 - 264 VAC (universal) or 120 - 370 VDC. With efficiency up to 94%, the series has an operating ambient temperature range -30°C to +70°C.

www.belfuse.com

DC-DC Step-Up Converter for Efficient Energy Harvesting Applications

Asahi Kasei Microdevices (AKM) has launched a DC-DC step-up converter with ultra-low power consumption that is able to boost low voltages, offering solutions for remote and battery-free operation as well as low-maintenance applications in the fields of asset monitoring and IoT. The AP4473 is a DC-DC step-up converter featuring the capability of boosting an input voltage of as low as 15 millivolts (mV) while maintaining an ultra-low power consumption of only 26 nanoamperes (nA). This single-chip solution allows electricity generation from a minimal thermal energy source, such as body heat, while enabling overcharge prevention and power supply control with minimal energy consumption.

In addition to the boost circuit, the device incorporates a PMOS switch and two hysteresis comparators. The switch disconnects the energy storage devices, such as capacitors, from the system, while its comparators automatically start and stop supplying power to the system. This makes it possible to configure a power supply unit in an energy harvesting system with a minimal number of passive elements, contributing to size and cost reductions for the overall system.

The AP4473 is suitable for applications in beacons for asset tracking and asset monitoring, environmental monitoring and IoT sensor nodes, as well as smartcards or IoT devices.

www.akm.com

LCC Design Tool Enables Highly Efficient LED Driver Design

Infineon Technologies introduces the LCC design tool, aiming to make a highly efficient yet complex design topology such as PFC plus LLC accessible to a broad LED driver manufacturer community at no additional cost. PFC plus LCC topology is 5 to 6 percent more efficient than other commonly used two-stage topologies. However, the design of LED drivers with this topology is highly time-consuming. Infineon's LCC tool, which is a novelty in the market, makes the design work much faster and easier.

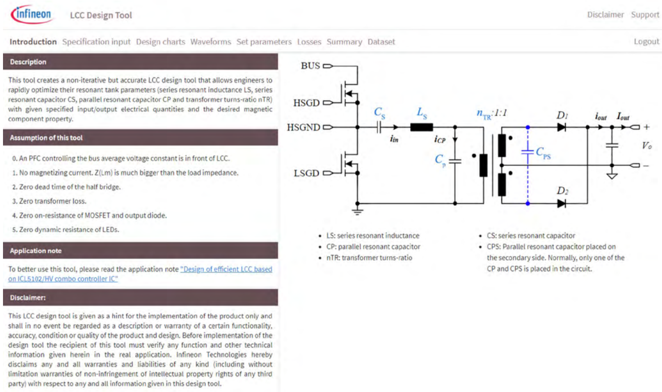

"Our LCC design tool offers a streamlined solution for designers to deploy highly efficient and reliable PFC plus LLC solutions in reduced time and effort, bypassing a time-consuming iterative design approach," said Hakan Yilmazer, Head of Application Management Lighting at Infineon Technologies. "Assuming that 300 million LED drivers with an average power of 60 W were converted from less efficient topologies to PFC plus LCC topology, the energy produced by one large coal power plant with a capacity of 1000 MW could be saved per year. This is now possible with the support of Infineon's LCC tool as well as the broad portfolio of suitable controllers and power switches."

www.infineon.com

Load Switches with Slew Rate Control

The GLF112x and GLF122x Series of 1A-rated load switches feature an operating temperature range (40ºC to +85ºC), integrated slew rate control, low RON (52mΩ), ultra-low IQ (1nA) and ISD (10nA) at 5.5V VIN. Built on GLF's proprietary load switch technology, they boast package reducing board space and allowing engineers and architects to have fewer design constraints. Target applications include wearables, IoT, medical devices (e.g., hearing aids), true wireless stereo (TWS), mobile phones, contactless payment systems, Bluetooth low energy (BLE) and other low power sub-systems.

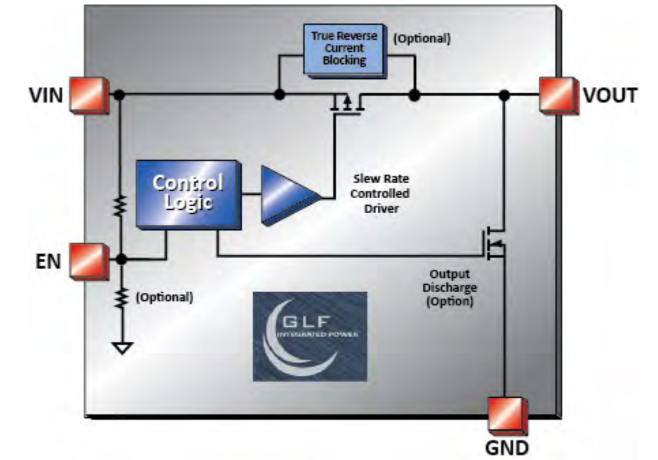

GLF122x load switches also provide True Reverse Current Blocking (TRCB), designed to cut off current flow if the V_{OUT} pin voltage exceeds V_{IN}. "GLF112x/GLF122x expands GLF load switch product family by offering the smallest size in the industry," said Eileen Sun, President and CEO at GLF Integrated Power. "The low IQ and ISD of the GLF112x and GLF122x Families help designers to reduce parasitic leakage current, improve system efficiency and increase battery lifetime, improving the overall user experience."

www.glfipower.com

Current Sensor for High-Power EV Traction Inverters

Distance and speed of charging are vital in the competitive EV sector and, like all vehicle components, high-power integrated traction inverters – which convert DC into AC and capture energy for the vehicle – need to combine superior performance with being as small and light as possible. Measuring just 29mm x 21mm x 12mm and weighing 27g, LEM's HSTDR current sensor is significantly more compact than a traditional C-core sensor, making it much easier to be integrated into space-limited inverter boxes.

The sensor enables traction inverters to operate at maximum efficiency by combining high accuracy with affordability and the ability to operate in demanding environments (the sensor has an operating range of -40°C to +125°C and is robust enough to cope with vibrations up to 10G). Using open loop Hall effect technology and an innovative magnetic core design, the HSTDR offers excellent immunity against external field and cross talk as well as consistent behaviour over frequency with little part-to-part phase shift dispersion, ensuring more accurate torque control.

What makes the sensor unique is not only that it is 42% smaller than its predecessor (LEM's HSNDR) but also weighs 50% less and offers 50% greater measuring range, as well as best-in-class accuracy and a global error over temperature and lifetime below 3.5%. Giving EV manufacturers the choice of having different current measuring ranges in the same housing – from ±300 A up to ±1500 A

– the sensor ensures galvanic separation between the primary circuit (high power) and the secondary circuit (electronic circuit), which is also suitable for 800V battery systems.

www.lem.com

High Power Linear Rack & Benchtop Power Supplies

Acopian launched their high power linear Infinity Rack and Benchtop power supplies rated up to 1200W. DC single/nominal output voltages range from 3.3VDC to 150VDC and up to 150A (1200W). All voltages are available in 2U, 3U and 4U high configurations. These linear power supplies are highly configurable. Standard features include, but are not limited to remote sensing, open sense protection, isolated output, internal EMI filtering, no minimum load requirements, short circuit and overload protection with enhanced surge capabilities, front panel AC input power switch with indicator, overtemp protection on heat sinks and thermostatically controlled fans.

Optional features include selecting your desired AC input voltage, Voltage Output Adjust and Current Limit Adjustments, Inhibit or Enable, Voltage and Current Monitoring, Latching Overcurrent control, Ethernet/USB/RS232/RS485 Digital Interfaces, Output blocking protection diode, High Frequency pulsed load filtering, Series Operation Diode capability, Alarm with Relay Contacts Options, Front Panel Mounted LED Output Indicator, Temperature monitor, handles, chassis slides, Digital Voltage and Current Meters and more. Linear operation minimizes output noise so these power supplies are ideal for use in test equipment, analog systems, controls, medical, aviation and R&D applications.

www.acopian.com

Dual-Channel Optocoupler Phototransistor

Würth Elektronik has expanded its WL-OCPT optocoupler product family with the DIP-8 design. Two-channel optocoupler phototransistors with eight pins are now available. This design contains two circuits inside a single component constructed from two input LEDs and two output phototransistors, therefore two separate circuits can be controlled with a single component. WL-OCPT features a stable current transfer ratio (CTR) over the entire operating temperature range (-55 to +110°C). The DIN-EN-60747-5-5-certified components have an insulation voltage of 5000 V, a collector-emitter voltage of 80 V, and a maximum forward current of 60 mA.

The Würth Elektronik optocouplers are suitable for optical and space-saving galvanic isolation in power supplies, chargers, computers, microprocessors, instruments, machines, ammeters or smart meters. Binning of the dual-channel WL-OCPT is in a CTR range of 130-400%, tested at an input current of 5 mA and a collector-emitter voltage of 5 V. Depending on the land pattern on the PCB, the DIP-8 optocoupler packages are available in standard, M, S and SL leadframe variants. The lead frames are made of copper thus guaranteeing the best solderability. Like all other WL-OCPT series optocouplers, the DIP-8 variants are now available from stock without a minimum order quantity. Developers receive free samples on request.

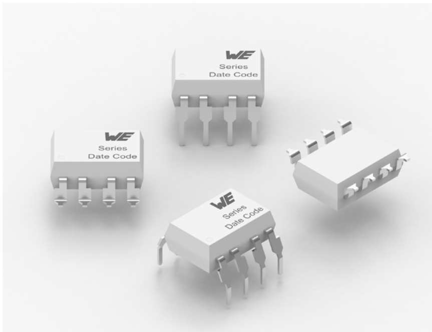

www.we-online.com

Planar Transformer Series Engineered for High Frequency, Smaller Space DC-DC Conversion Designs

Bourns introduced its Model PLN0xx-ED21 Series Planar Transformers with the advanced features needed to meet today's high frequency, smaller space power conversion application requirements. These forward converter transformers are designed to deliver high volumetric power density, low loss and efficiency in a compact, low-height profile design. Bourns® Model PLN0xx-ED21 Series Planar Transformers also are designed for greater reliability due to their enhanced thermal conduction and heat dissipation properties.

The advent of planar-style transformer components increases design flexibility and offers efficiency and power density advantages over conventional wirewound transformer designs due to reduced AC resistance losses. Providing from 48 watts up to 70 watts of output power in applications with input voltages ranging from 33 to 57 VDC and a switching frequency of 250 kHz, Model PLN0xx-ED21 Series planar transformers have low leakage inductance from 0.29µH to 0.60 µH and a volt-second time of 81.6 (V-µsec). The series offers 33 V to 57 V input voltage, 5 V to 12 V output voltage at 4 to 14 A output with various turns ratios. These features and their compact design make Bourns® Model PLN0xx-ED21 Series planar transformers ideal power conversion solutions for high density industrial power systems, low profile Switched-Mode Power Supplies

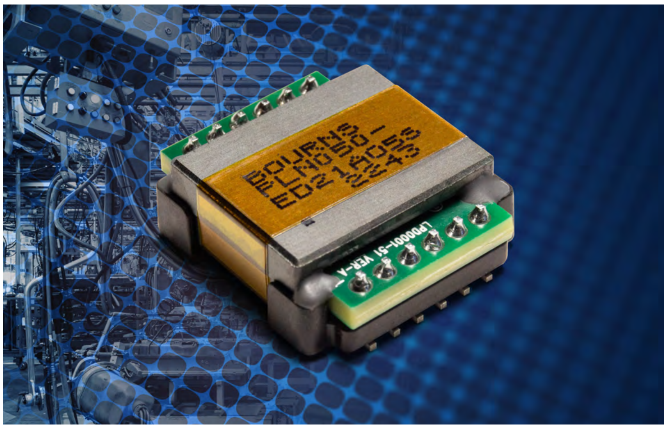

(SMPS), LED lighting applications, Battery Management Systems (BMS), PoE applications, and many other forward transformer applications. These planar transformers from Bourns use standard PWB material for the transformer windings, soldered to an SMT header to create a simple-to-use, surface mount component that helps ease assembly.

www.bourns.com

200 V, 10 mΩ GaN FET Joins Family of Footprint Compatible QFN Packaged Devices

EPC introduces the 200 V, 10 mΩ EPC2307 in a thermally enhanced QFN in a tiny 3 mm x 5 mm footprint. The EPC2307 is footprint compatible with the previously released 100 V, 1.8 mΩ EPC2302, the 100 V 3.8 mΩ EPC2306, the 150 V, 3 mΩ EPC2305, the 150 V, 6 mΩ EPC2308, and the 200 V, 5 mΩ EPC2304 allowing designers to trade off RDS(on) vs. price to optimize solutions for efficiency or cost by dropping in a different part number in the same PCB footprint.

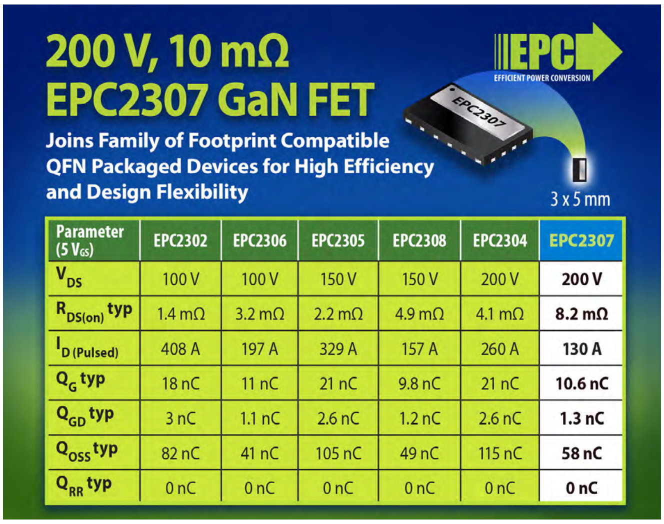

Parameter (5 V_{GS})	EPC2302	EPC2306	EPC2305	EPC2308	EPC2304	EPC2307
V_{DS}	100 V	100 V	150 V	150 V	200 V	**200 V**
$R_{DS(on)}$ typ	1.4 mΩ	3.2 mΩ	2.2 mΩ	4.9 mΩ	4.1 mΩ	**8.2 mΩ**
$I_{D\,(Pulsed)}$	408 A	197 A	329 A	157 A	260 A	**130 A**
Q_G typ	18 nC	11 nC	21 nC	9.8 nC	21 nC	**10.6 nC**
Q_{GD} typ	3 nC	1.1 nC	2.6 nC	1.2 nC	2.6 nC	**1.3 nC**
Q_{OSS} typ	82 nC	41 nC	105 nC	49 nC	115 nC	**58 nC**
Q_{RR} typ	0 nC	0 nC	0 nC	0 nC	0 nC	**0 nC**

The devices feature a thermally enhanced QFN package with exposed top. The extremely small thermal resistance improves heat dissipation through a heatsink or heat spreader for excellent thermal behavior, while wettable flanks simplify assembly, and footprint compatibility offers design flexibility to specs change for fast time to market. This family of devices bring several benefits to motor drive designs including very short deadtimes for high motor + inverter system efficiency, lower current ripple for reduced magnetic loss, lower torque ripple for improved precision, and lower filtering for lower cost.

For DC-DC conversion applications, these devices offer up to five times higher power density, excellent heat dissipation, and lower system costs in both hard switching and soft switching designs. Additionally, ringing and overshoot are both significantly reduced for better EMI.

www.epc-co.com

DC/DC Converters for Data-Hungry Applications

Helping to enable the next generation of high-performance, computing-intensive technologies, ABB Power Conversion introduced its DLynx IIITM point-of-load (POL) modules, the third generation of its proven digital DLynx family. The high-current modules enable board design flexibility by implementing a master-satellite concept to help meet the needs of today's networking, data center, and industrial equipment, including the latest application-specific integrated circuits (ASICs) and field-programmable gate arrays (FPGAs).

The DLynx III product family includes 40-, 80-, 120-, and 160-amp (A) master DC/DC converters as well as 40A and 160A satellite modules. The master DC/DC converters can be used as standalone POL modules or can be used in tandem with satellites modules. When used together, the master and satellite modules can be deployed in higher-powered single-output configurations to meet growing board-level power requirements and power density demands or in dual-output configurations to power components with differing output voltage requirements.

"As networking and data center equipment continues to evolve to meet the need for higher computing capacities and more data throughput at faster speeds, the components powering this advanced equipment must also evolve," said Vito Savino, data center and wireline segment leader for ABB Power Conversion. "When looking to pack more computing prowess onto printed circuit boards with fixed board footprints, every millimeter of available space becomes premium real estate."

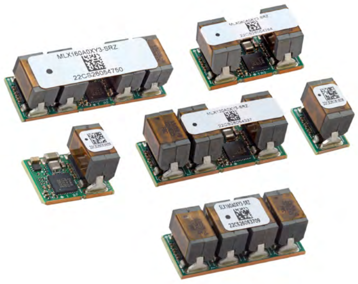

www.abbpowerconversion.com

In-Vehicle Network ESD Protection Portfolio for 24 V Board Net Systems

Nexperia introduced an AEC-Q101 qualified portfolio with six ESD protection devices (PESD2CANFD36XX-Q), designed to protect bus lines in automotive in-vehicle networks (IVN) such as LIN, CAN, CAN-FD, FlexRay and SENT from damage caused by electrostatic discharge (ESD) and other transients. As data rates increase and vehicles feature more electrification, the need for ESD protection is becoming ever more critical. Providing the right protection for automotive modules is a continuous challenge for design engineers.

In contrast to the battery voltage found in cars and smaller vehicles, 24 V board nets are typically used in trucks and commercial vehicles. ESD protection devices with operating voltages typically above 32 V are required to safeguard sensitive signal lines in 24 V board nets. Addressing these requirements, Nexperia has designed this portfolio to have a maximum reverse standoff voltage of 36 V and up to 22 kV ESD protection. This performance is combined with a low clamping voltage of VCL= 48 V at IPP = 1 A to provide the best-in-class system-level robustness for IVN.

Keeping the specifications of in-vehicle networks and the ease of design in mind, Nexperia is offering this portfolio in SOT23 and SOT323 packages with three different ultra-low capacitance classes of 4.3 pF, 6 pF and 10 pF, which help ensure a smooth communication between interfaces without impacting signal integrity. This combination maximizes flexibility in PCB design and offers several performance options for design engineers.

www.nexperia.com

High Power Density 700W Power Supplies for Medical and Industrial Applications

COSEL announced the introduction of its open-frame high power density, 700W, 3x5 inch power supply optimized for efficient cooling for use in demanding medical and industrial applications. Based on the robust platform with optimized thermal conduction, the GHA700F delivers 700W within a 3"x5" industry footprint. With a power density of 31.1W per cubic inch it's one of the highest power density power supplies in its category for powering medical and industrial applications. The GHA700F is designed in accordance with safety standard IEC 60601-1, making it suitable for Body Floating medical applications but its high isolation and creepage distance make it eminently suitable for demanding industrial applications, complying with EN61558-2-16 (OVC III) and simplifying design to conform to EN60335. To power a large range of systems-bus-voltages the GHA700F is available in four output voltages, 24, 30, 48 and 56VDC and has a universal input voltage of 85 to 264VAC. Using the latest power switching topology and components, the GHA700F boasts an excellent efficiency figure of up to 96%. With the growing number of medical applications operating in low noise environments, equipment manufacturers are optimizing equipments to operate with limited airflow. To meet such requirements, power supplies must be design-optimized to combine conduction and convection cooling, offering systems designers the possibility to best optimize the placement of the power supply, without compromising performance.

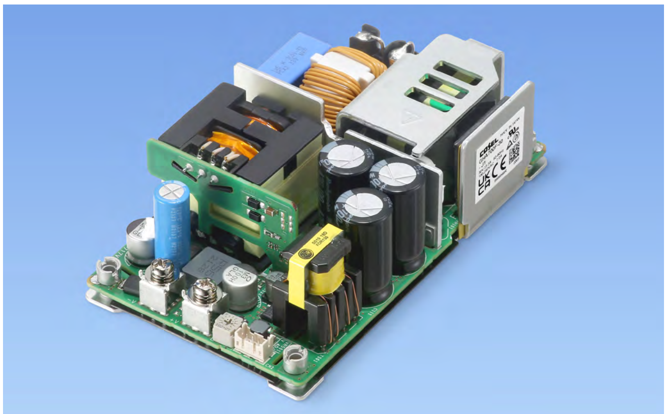

www.coseleurope.eu

SiC SBDs for Data Center PSUs

ROHM has announced that Murata Power Solutions is using its silicon carbide (SiC) Schottky Barrier Diodes (SBD) to increase performance and reduce the size of Power Supply Units (PSUs) for data center applications. ROHM's SiC SBDs, SCS308AH feature high surge resistance and short recovery time, enabling high-speed switching. Murata's D1U front end AC-DC power supply series include many active units such as the D1U54P-W-2000-12-HB3C and D1U54P-W-1200-12-HC4PC, highly-efficient power-factor-corrected front-end power supplies that provide 12V main and 12V/3.3V standby output. Multiple units can share current and operate in parallel. The power supplies support hot-plugging and are protected from fault conditions such as over-temperature, over-current and over-voltage. What's more, the low profile 1U package make them ideal for delivering reliable, efficient power to servers, workstations, storage systems and other 12V distributed power systems while minimizing the number of required power modules.

Jay Barrus, President, ROHM Semiconductor U.S.A.:

"We are excited to help Murata Power Solutions, a Murata Manufacturing Group company that leads the industry in the field of industrial equipment including power supply systems. We are the leading company in SiC power semiconductors and have achieved a significant technological lead in this field along with the provision of power solutions combined with gate driver ICs.

Together with Murata Power Solutions, we want to further improve the energy efficiency of power supply systems by using the full potential of SiC technology for industrial and data infrastructure."

www.rohm.com

Prismatic Supercapacitor for Space-Constrained IoT and Batteryless Devices

CAP-XX has launched its DMV750 2.2mm prismatic 3V supercapacitor to provide high performance for IoT, medical and other space-constrained and mission-critical electronic devices. This multi-purpose 3V prismatic supercap can support the industry's common 3V coin cell battery to extend its life and functionality, replace a bulky 3V cylindrical supercap to save design space, or replace batteries altogether when micro energy harvesting can extract enough solar, vibration, RF or other environmental energy to charge the ultra-efficient supercapacitor in sustainable batteryless devices.

Packing 23% more energy than a 2.7-volt supercap in the same size package, the 3V,

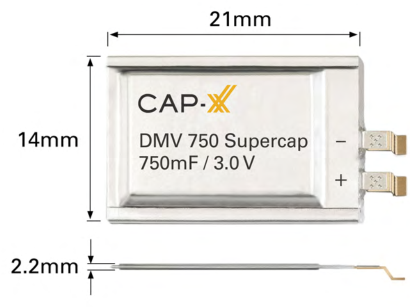

DMV750 supercap provides high peak pulse power to enable either batteryless or more battery-efficient applications. It measures 21 millimetres x 14 millimetres x 2.2 millimetres, and operates from -20°C to +85°C.

"It is estimated that over 5 billion 3V coin cell batteries and 12 billion IoT devices are sold annually," explained Anthony Kongats, CEO at CAP-XX. "While not all devices will require a supercapacitor, a large number would benefit from using our powerful DMV750 supercapacitor to store and release the energy needed for peak power functions like data transmission."

Kongats continued, "Our DMV750 ultra-thin prismatic 3V supercap provides design engineers with multiple options to overcome power delivery challenges in space-constrained, mission-critical and sustainable electronic devices."

www.cap-xx.com

Integrated GaN System-in-Package for USB-C PD Adapters and Other Low Power Applications

Transphorm and Weltrend Semiconductor announced the release of their first GaN System-in-Package (SiP). The WT7162RHUG24A is an integrated circuit designed for use in 45 to 100 watt USB-C PD power adapters charging smartphones, tablets, laptops, and other smart devices. It offers peak power efficiency of greater than 93%.

Weltrend transphorm

“The WT7162RHUG24A is the industry’s first publicly announced SiP using Transphorm GaN. It enables manufacturers to develop a less expensive system solution given fewer components are required and a smaller PCB can be used among other advantages. It also reduces system development time. Effectively, we’re removing design barriers for adapter manufacturers,” said Tony Lin, President, Weltrend. “Notably, this product also allows Weltrend to move into a new market. It is the first-ever SiP for our PWM controllers, validating our commitment to supporting high volume growth sectors. And, with the integration of the GaN FET, we’ve raised the level of performance output. A win for Weltrend, Transphorm, and our mutual customers.”

“The adapter fast charger market is a fast growing segment for GaN adoption today. We are gaining market share and continue to innovate, most recently with this GaN SiP, which allows for even easier use of our GaN devices,” said Primit Parikh, President and COO, Transphorm. “We’re excited to integrate our industry leading SuperGaN platform with Weltrend’s innovative adapter power controller technology. Weltrend has delivered a leading power conversion platform which creates a simple-to-use solution for adapter/fast charger customers that both companies can use to accelerate wins in this market.”

www.weltrend.com

AC-DC Active Bridge Rectifier Solution

Alpha and Omega Semiconductor introduced an extension to its active bridge driver, AlphaZBL™ family. Available in an SOP-8L package, the AOZ7203AV is a self-powered dual driver IC for driving external high-voltage MOSFETs to replace two low-side diodes of bridge rectifier. The device is suitable for use in adapters for high-end laptops and televisions, as well as power supplies for Desktops, Game Consoles, and Servers.

The AOZ7203AV features a high withstand voltage, a self-powered Vcc supply from the AC line, ultra-low operation current, and X-capacitor discharge (CB safety certified). A break-before-make circuit avoids the overlap of two gate driving while driving the low-side high voltage MOSFETs in an active bridge rectifier circuit. With an input voltage of up to 600V, the AOZ7203AV has a wide operating (-40°C to +125°C) ambient temperature range and driving low RDSON HV MOSFETs to gain more efficiency improvement of AC power supply. These features make the AOZ7203AV an optimal solution for efficient replacement of lossy diodes in the bridge rectifier circuit of an AC-DC power supply.

www.aosmd.com

Single-Chip Intelligent Battery Management Solutions for 20-Cell Systems

Qorvo announced it has expanded its power management portfolio to include the PAC22140 and PAC25140 Power Application Controller® (PAC) devices. The two PACs are the single-chip solutions to offer support for battery packs with up to 20 cells in series (20s). These products leverage an intelligent motor control foundation to enable intelligent battery management solutions (BMS) for a wide range of industrial, e-mobility and battery backup applications.

The highly integrated PAC22140 and PAC25140 save designers more than 50% of PCB space and lower total BOM cost by 30%, while reducing time to market leveraging Qorvo's hardware and firmware ecosystem. The devices integrate all essential analog and power management peripherals with a 32-bit Arm® Cortex® M0 or M4F microcontroller and include cell balancing, monitoring and protection for 10s-20s battery packs.

The PAC22140 and PAC25140 provide access to multiple analog and digital peripherals required to manage today's high-cell-count battery packs. These include a programmable-gain differential amplifier, multiple 16-bit Sigma-Delta ADCs for current and voltage sensing, and a 10-bit SAR ADC. A single-supply 145V-buck DC/DC controller generates a 5V system rail to power the device, while an integrated charge pump supports the charge and discharge FET drivers.

"The need for higher cell count solutions is increasing as end users demand longer battery life, faster charging time and lighter overall weight from new battery-powered applications," said Brian McCarthy, senior manager for Qorvo's PAC product line. "The highly integrated PAC22140 and PAC25140 provide designers complete solutions for these high-power, high-performance systems."

www.qorvo.com

Advertising Index

Alpha & Omega	31	EPC	C4	Mitsubishi Electric	33
Battery Show Europe	32	Finepower	C3	PCIM Asia	63
CISSOID	35	Fuji Electric Europe	11	PCIM Europe	57
Coilcraft	25	GvA	21	Plexim	37
COMSOL	17	HIOKI	13	Qorvo	27
Cornell Dubilier	19	Hitachi	9	ROHM	7
CWIEME Berlin	55	Hitachi Energy	39	Sensor + Test	49
Danisense	45	Infineon	23	TAMURA	53
Dean Technology	47	Innoscience	43	Texas Instruments	41
ed-k	C2	ITG Electronics	15	Vincotech	29
Electronic Concepts	1	LEM	5	Würth Elektronik eiSos	3
EM Power	59	Magnetic Metals	51		

Invitation to PCIM
May 9 –11, 2023

pcim EUROPE

Finally, it`s time again!
The gates of the important trade fair for power electronics in Germany are opening and we will join!

The entire Finepower team is looking forward to welcome you personally. Since the trade fair management has changed the allocation of free visitor vouchers, unfortunately, we cannot provide you with a code at this point. The number of free codes has also been limited by Mesago, so please don't wait too long. To receive a personal voucher code, please send an email to:
marketing_contact@finepower.com
If you need several codes, please indicate this in the mail.

All members of Finepower are looking forward seeing you again and to exciting discussions.
Your Finepower - Team

hall 9 / booth 321

www.finepower.com